MR Imaging of Benign Focal Liver Lesions

Jonathan R. Cogley, MD[a], Frank H. Miller, MD[b,*]

KEYWORDS

• Liver • Hepatic MR imaging • Diffusion-weighted imaging • Hemangioma
• Focal nodular hyperplasia (FNH) • Hepatic adenoma • Liver abscess • Biliary cystadenoma

KEY POINTS

- Magnetic resonance (MR) imaging is helpful for definitive characterization of various solid and cystic hepatic lesions.
- MR imaging also provides important information about the background liver parenchyma, biliary tree, and hepatic vasculature.
- Diffusion-weighted imaging in the liver can be particularly helpful for detection of otherwise subtle lesions and for the diagnosis of pyogenic abscesses.
- Diffusion-weighted imaging alone cannot differentiate between solid benign hepatocellular lesions and malignant lesions, as both can exhibit restricted diffusion with overlap between their respective apparent diffusion coefficient values.
- Hepatocyte-specific contrast agents are helpful for the differentiation of focal nodular hyperplasia and hepatocellular adenoma, two lesions with overlapping imaging features and patient populations, but with potential management implications depending on the diagnosis.

INTRODUCTION

Focal liver lesions are increasingly encountered during routine imaging studies because of advances in technology and more widespread use of imaging. The great majority of lesions are benign in patients with noncirrhotic livers; however, many are indeterminate at the time of initial discovery. Definitive characterization by magnetic resonance (MR) imaging may alleviate patient anxiety, drastically alter management in someone undergoing staging for malignancy, and help avoid unnecessary biopsy or costly follow-up imaging.

MR imaging offers important advantages over computed tomography (CT), such as the lack of ionizing radiation and improved soft tissue contrast. The American College of Radiology Appropriateness Criteria[1] assigns the highest rating to MR imaging without and with contrast for characterization of indeterminate liver lesions, regardless of whether the patient is otherwise healthy, has liver disease, or has a known extrahepatic malignancy. This review presents a standardized approach to liver MR imaging while detailing common and less common benign focal liver lesions and their imaging characteristics.

MR IMAGING TECHNIQUE

Protocol

The goal of a dedicated liver MR imaging is to fully assess any focal lesions and provide valuable information about the background liver parenchyma, biliary system, and vasculature. This is

Funding Source: None.
Conflict of Interest: None.
[a] Section of Body Imaging, Department of Radiology, Northwestern Memorial Hospital, Northwestern University Feinberg School of Medicine, 676 North Saint Clair Street, Suite 800, Chicago, IL 60611, USA; [b] Department of Radiology, Northwestern University Feinberg School of Medicine, Chicago, IL 60611, USA
* Corresponding author.
E-mail address: fmiller@northwestern.edu

Radiol Clin N Am ■ (2014) ■–■
http://dx.doi.org/10.1016/j.rcl.2014.02.005
0033-8389/14/$ – see front matter

accomplished by using a wide range of fluid-sensitive and anatomic pulse sequences, including dynamic contrast-enhanced images that allow for improved lesion detection and characterization (Table 1). Enhancement depends on both the nature of the lesion and timing of imaging with respect to the contrast bolus.[2] Images are routinely obtained during hepatic arterial, portal venous, and equilibrium (equal distribution of contrast among the intravascular and extravascular extracellular compartments) phases. Magnetic resonance cholangiopancreatography (MRCP) images can be obtained to better evaluate the biliary tree. Patient cooperation with breath-holding instructions is required to achieve high-quality images.

Contrast Agents

Gadolinium contrast agents have strong paramagnetic effects that shorten predominately the T1 relaxation times of tissues, leading to increased signal intensity (enhancement) on T1-weighted images.[3] The 2 main categories of contrast agents used for liver MR imaging are (1) extracellular and (2) hepatocyte-specific. Extracellular contrast agents are more widely used, providing information on the pattern and degree of enhancement analogous to iodinated contrast agents for CT. After intravenous injection, they circulate the vascular system and are distributed into extracellular spaces before undergoing renal excretion. Hepatocyte-specific contrast agents provide this extracellular dynamic information plus unique additional delayed phase information. On delayed images, tumors of hepatocellular origin with functioning hepatocytes and biliary excretion take up and retain hepatocyte-specific contrast to some degree, whereas other lesions generally do not. This allows for better characterization of focal liver lesions and potentially increases the detection of small lesions that would otherwise be missed.[2]

Table 1
Example of comprehensive liver MR imaging protocol

Protocol Step	Sequence
Precontrast images	T2-weighted single-shot fast SE T1-weighted in and opposed phase GRE Diffusion-weighted imaging T2-weighted FS fast SE 3D T1-weighted FS spoiled GRE T2-weighted MRCP (optional)
Postcontrast images	Dynamic 3D T1-weighted FS spoiled GRE (in hepatic arterial, portal venous, and equilibrium phases) Delayed hepatocyte phase (if applicable)

Abbreviations: FS, fat-suppressed; GRE, gradient echo; MRCP, MR cholangiopancreatography; SE, spin echo; 3D, three-dimensional.

Hepatocyte-specific contrast agents currently approved for clinical use by the Food and Drug Administration are gadobenate dimeglumine (MultiHance; Bracco Diagnostics Inc, Princeton, NJ) and gadoxetate disodium (Eovist; Bayer HealthCare, Wayne, NJ; marketed as Primovist in Europe). In a patient with normal liver and renal function, gadoxetate disodium has a much greater percentage of biliary excretion (50%) than gadobenate dimeglumine (3%–5%).[4] Therefore, more intense liver enhancement and earlier hepatocyte-phase imaging is achieved with gadoxetate disodium (usually within 20 minutes) than gadobenate dimeglumine (usually performed after 60–90-minute delay).[2,3] T2-weighted and diffusion-weighted images can be obtained after injection of gadoxetate disodium to improve time efficiency.

The FDA-approved, manufacturer-recommended dose of gadoxetate disodium (0.025 mmol/kg) is only one-fourth that of gadobenate dimeglumine and extracellular contrast agents (0.1 mmol/kg), resulting in a relatively weaker T1 shortening effect.[2] A smaller volume of contrast (prefilled 10-mL syringe) is typically administered. If injected at a rate of 2 mL/s, it may take less time to deliver the contrast bolus than it does to complete a single high-quality data acquisition.[4] Consequently, it can be challenging to capture peak arterial phase enhancement. Shortened scanning times or reduced injection rates of 1 mL/s have been proposed to overcome this temporal mismatch.[4] Additional methods to avoid missing peak arterial phase include using a bolus timing technique, such as automated bolus detection algorithm or fluoroscopic triggering, or obtaining multiple consecutive arterial phase data sets with higher temporal but lower spatial resolution.[4,5]

Diffusion-Weighted Imaging

Diffusion-weighted imaging (DWI), a technique that derives image contrast from differences in random motion of water molecules, has become a standard part of abdominal MR imaging protocols in recent years. The underlying principle is that different biologic tissues exhibit varying levels of restricted water diffusion, dependent on such factors as tissue cellularity and cell membrane integrity.[6] The ability to depict areas of high

cellularity can be helpful in hepatic lesion detection and characterization in a noninvasive manner. DWI does not rely on intravenous gadolinium; therefore, its use is particularly attractive in patients with poor renal function who cannot receive contrast because of the potential risk of nephrogenic systemic fibrosis.[7]

In general, DWI uses a fast single-shot echo-planar imaging-based sequence. Images at our institution are obtained at 3 different b-values (ranging from low to high) to calculate an apparent diffusion coefficient (ADC) map. Low b-value (ie, 50 s/mm^2) or "black blood" diffusion images result in improved lesion detection owing to suppression of bright signal from vessels or periportal tissue and lack of motion blurring compared with standard T2-weighted turbo spin-echo (TSE) and single-shot TSE images.[8–10] In our experience, subtle or small additional lesions easily overlooked on conventional MR images may be much more conspicuous on low b-value diffusion images. Higher b-value (ie, 500 and 800 s/mm^2) images provide more diffusion information and help with lesion characterization. Common benign liver lesions generally have higher ADC values than malignant lesions. This may allow for quick differentiation of a hepatic cyst or hemangioma from a solid hepatocellular mass or metastasis. However, overlap exists between ADC values of solid benign hepatocellular lesions, such as focal nodular hyperplasia (FNH) or hepatocellular adenoma (HCA), and those of malignant lesions.[7,10–15] Thus, information provided by DWI needs to be interpreted in conjunction with lesion morphology and signal characteristics on other sequences.

FOCAL LIVER LESIONS

Hemangioma

Hemangioma is the most common benign liver tumor, with a reported prevalence as high as 20%.[16–18] Most hemangiomas (60%–80%) are diagnosed in adults between 30 and 50 years of age.[19] There is a clear female predominance (2:1 to 5:1 ratio).[20] In most cases, hemangiomas are discovered incidentally and are of no clinical consequence. Accurate diagnosis is critical to avoid unnecessary further workup, including biopsy.

The gross and histologic features of hemangiomas lend to their characteristic appearance at MR imaging. Hemangiomas consist of numerous vascular channels, each lined with a single layer of epithelial cells and separated by fibrous septae.[21] They are usually well defined, often round or mildly lobulated. Due to the long T2 relaxation time of their blood-filled spaces, hemangiomas demonstrate T2 hyperintense signal classically described as "light bulb bright" or isointense to cerebral spinal fluid (CSF).[16] They are often slightly less T2 hyperintense than simple cysts or CSF on single-shot TSE images. Nevertheless, this T2 hyperintense signal is one of the most reliable findings in diagnosing hemangiomas.[22] They appear hypointense to adjacent liver on T1-weighted images. Following contrast, a pattern of discontinuous peripheral nodular enhancement with progressive, centripetal filling on more delayed images is characteristic (**Fig. 1**).[23]

Incomplete filling by contrast is common in hemangiomas larger than 3 cm due to central scarring. This is especially true for "giant" hemangiomas, a term generally reserved for lesions larger than 5 cm, which may also enhance asymmetrically because of regions of thrombosis.[24] In giant hemangiomas, irregular or "flame-shaped" discontinuous peripheral enhancement may dominate or coexist with the typical nodular enhancement pattern seen in smaller hemangiomas.[21] They also may look more complex on T2-weighted images, sometimes with a multiloculated appearance resulting from a network of hypointense septae or with a central T2 hyperintense cleft, which may be from cystic degeneration or liquefaction (**Fig. 2**).[20,21]

Conversely, some small (<2 cm) hemangiomas show rapid complete filling on the arterial-phase images. They are typically high signal intensity on T2-weighted images. These small lesions, referred to as "flash-filling" hemangiomas, are often associated with adjacent arterioportal shunting, most commonly seen as a wedge-shaped subcapsular area of transient hyperenhancement during the arterial phase (**Fig. 3**).[22,23] Segmental or lobar perfusional variants also can be seen in association with larger hemangiomas.

Most hemangiomas remain stable in size on follow-up imaging.[17] Larger lesions can sometimes be associated with symptoms related to mass-effect on adjacent structures. Other complications have occasionally been reported, most often with giant hemangiomas. These include intratumoral hemorrhage, inflammatory changes, or consumptive coagulopathy (Kasabach-Merritt syndrome).[24] Such complicated lesions may require aggressive management, such as arterial embolization or resection.

Rarely, hemangiomatous lesions can diffusely replace the liver parenchyma. In contrast to the sharp borders of classic hemangiomas, boundaries of so-called "hemangiomatosis" are ill defined. This pattern has been observed adjacent to giant hemangiomas (see **Fig. 2**B), and in some cases, can be a manifestation of

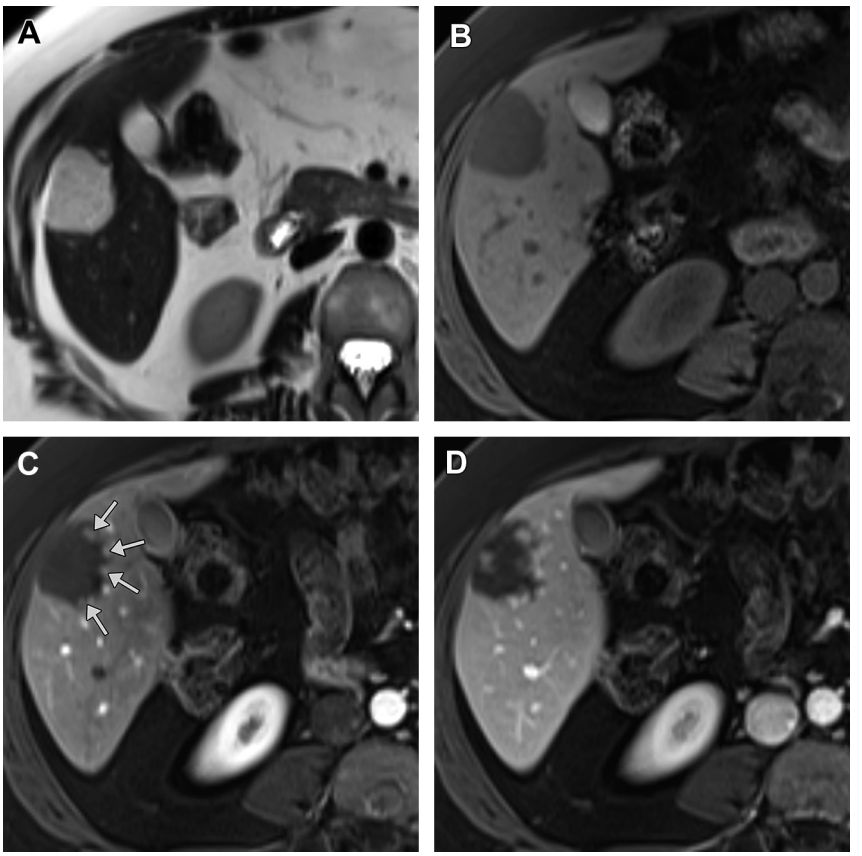

Fig. 1. Typical hemangioma. (*A*, *B*) A well-circumscribed mass demonstrates uniform T2 hyperintense and T1 hypointense signal. (*C*) Characteristic discontinuous peripheral nodular enhancement is seen during arterial phase (*arrows*). (*D*) Subsequent postcontrast images show progressive centripetal filling of the hemangioma.

systemic diseases, such as hereditary hemorrhagic telangiectasia.[25]

"Sclerosed" hemangiomas have predominately fibrosed and obliterated vascular spaces and may represent the end stage of hemangioma involution.[20] The typical imaging features of a hemangioma are altered or lost, making a prospective diagnosis challenging (**Fig. 4**). Hemangiomas can be especially difficult to diagnose in the setting of cirrhosis, where they are less common than in the general population and may sclerose. Doyle and colleagues[17] described features suggestive of sclerosed hemangiomas in a series of 10 lesions: geographic margins, volume loss with capsular retraction, adjacent wedge-shaped perfusional variant, nodular regions of internal enhancement (not necessarily in the periphery of the lesion), and presence of other more typical hemangiomas within the liver. All sclerosed hemangiomas in this series were T2 hyperintense to a variable degree; however, certain malignant lesions can also be T2 hyperintense. These include hypervascular metastases from a primary neuroendocrine tumor (pancreatic islet cell, carcinoid, or pheochromocytoma), breast cancer, renal cell carcinoma, thyroid cancer, melanoma, or sarcoma, in addition to cystic-appearing metastases from mucinous gastrointestinal malignancies.[22,26] Capsular retraction is not specific for "sclerosed" hemangioma; it also can be a feature of peripheral cholangiocarcinoma, epithelioid hemangioendothelioma, and liver metastasis.[20] Prior imaging should be evaluated to determine if the lesion had a more typical appearance of hemangioma previously.

Some hypervascular tumors or treated metastases can mimic peripheral nodular enhancement or show prolonged contrast enhancement (**Fig. 5**). The presence of an early complete (rather than discontinuous) rim of peripheral enhancement or "washout" of contrast on delayed images can help differentiate these metastatic lesions from hemangiomas.[22,26]

As gadoxetate disodium–enhanced MR imaging is increasingly used, it is important to recognize certain pitfalls that may arise with hemangiomas.

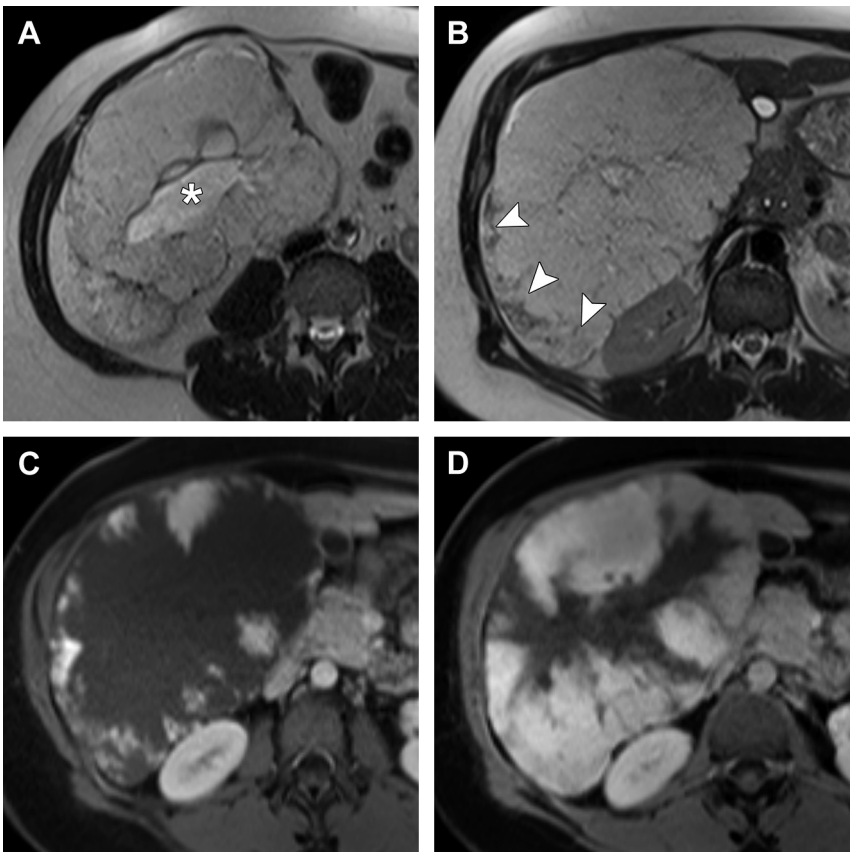

Fig. 2. Giant hemangioma. (*A*) Large T2 hyperintense mass with a central T2 hyperintense cleft (*asterisk*) from cystic degeneration or liquefaction. (*B*) Note the more ill-defined "hemangiomatosis" adjacent to its posterior border (*arrowheads*), a pattern that can be seen adjacent to giant hemangiomas. (*C*, *D*) Postcontrast images demonstrate characteristic peripheral discontinuous "flame-shaped" pattern of enhancement with progressive but incomplete centripetal filling on delayed images.

On 20-minute delayed hepatocyte-phase images, hemangiomas appear hypointense relative to the liver because they lack hepatocytes. However, the gradual process of contrast uptake by hepatocytes and removal from vascular spaces begins even earlier. Hemangiomas may appear hypointense relative to the increasingly bright background liver parenchyma as early as the equilibrium phase. With flash-filling hemangiomas, a resulting "pseudowashout" appearance can mimic hypervascular metastases (**Fig. 6**).[27] Furthermore, some small hemangiomas lack the typical enhancement pattern and can be firmly diagnosed only on delayed images when they appear isointense to blood pool. With gadoxetate disodium, delayed fill-in of these small atypical hemangiomas could be masked, making the diagnosis more difficult.[28] The typical high signal on T2-weighted images may be helpful in these cases. We try to use conventional gadolinium agents instead of gadoxetate disodium-enhanced MR imaging for the characterization of hemangiomas.

Focal Nodular Hyperplasia

FNH is the second most common benign liver tumor, with an estimated prevalence of 3% to 8%.[29] Most often found in young and middle-aged women, FNH can be seen across all age groups and also occurs in men.[30] A clear female predominance (8:1 ratio) suggests a role for endogenous or exogenous estrogens in its pathogenesis. Some investigators suggest a link between oral contraceptives and FNH because of reports of size regression following their withdrawal[29,31,32]; however, their potential influence is controversial. In one study of 216 women with FNH, Mathieu and colleagues[33] suggested that (1) neither size nor number of FNHs were influenced by oral contraceptives and (2) size changes during follow-up were rare and did not seem to depend on their use.

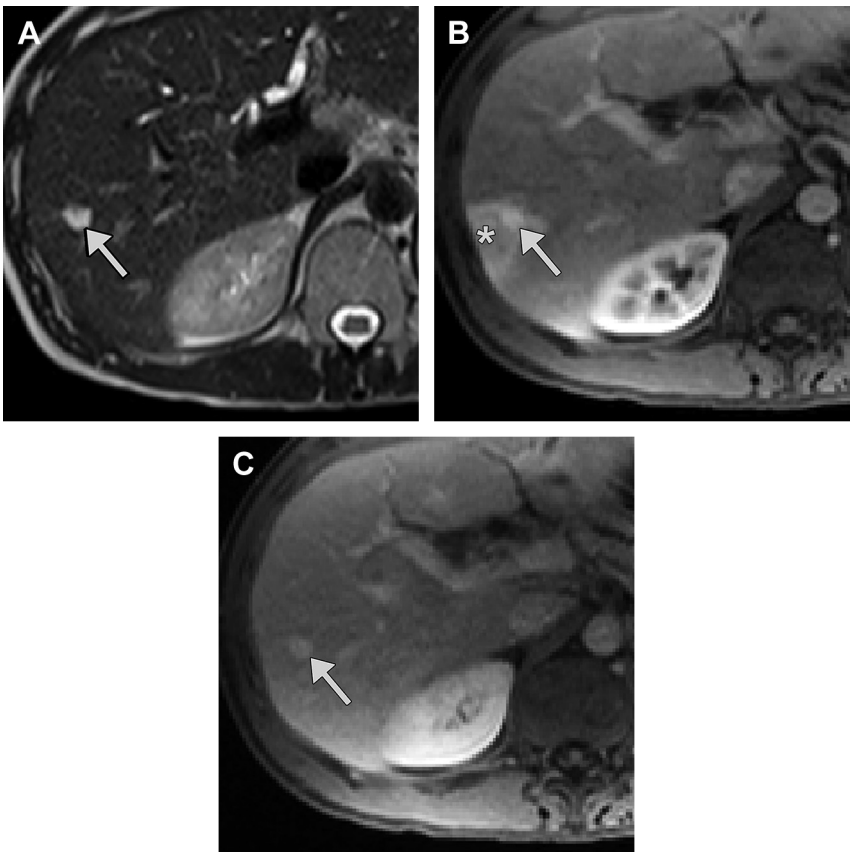

Fig. 3. Flash-filling hemangioma with associated perfusional variant. (*A*) A small well-defined T2 hyperintense liver lesion is present (*arrow*). (*B*) During arterial phase, this shows rapid complete filling by contrast (*arrow*). Note the adjacent wedge-shaped subcapsular region of transient hyperenhancement (*asterisk*). (*C*) The hemangioma (*arrow*) retains contrast on more delayed images, its signal intensity following that of blood pool.

FNH is usually a well-circumscribed, nonencapsulated mass less than 5 cm in diameter found in an otherwise healthy liver. The pathogenesis is not fully understood, but it is generally considered a hyperplastic response to a congenital or acquired vascular anomaly. Histologically, multiple small nodules composed of normal hepatocytes are clustered about a central scar of fibrous connective tissue. Characteristic pathologic findings include an enlarged feeding artery, numerous capillaries, and malformed biliary ductules. Generally, these lesions do not contain portal veins.[29]

FNH has been called a "stealth lesion" for being invisible on noncontrast CT; it is also isointense or nearly isointense to adjacent liver parenchyma on many MR imaging sequences (**Fig. 7**). FNH is typically homogeneous in signal intensity and appears isointense to slightly hypointense on T1-weighted images and isointense to slightly hyperintense on T2-weighted images.[30] A stellate central scar of T2 hyperintense signal (related to vascular channels, bile ductules, or edema) may be present, especially in lesions larger than 3 cm (**Fig. 8**).[29,30,34] Because its vascular supply is predominately arterial, FNH typically shows intense uniform enhancement during arterial phase.[34] The lesion usually fades to become isointense or slightly hyperintense to the liver on portal venous and equilibrium phases; if present, the central scar shows delayed enhancement. These typical features allow for a confident diagnosis based on imaging alone.

Because there is no evidence to support malignant potential of FNHs, and their associated complication rate is extremely low, management is conservative.[29] Only a minority of lesions require biopsy. Atypical findings that can be misleading include (1) heterogeneous T1 and T2 signal intensity, (2) hyperintense signal on precontrast T1-weighted images, and (3) hypointense signal relative to the liver during hepatic venous and equilibrium phases suggesting "washout."[29] Occasionally, FNH may exhibit a pseudocapsule

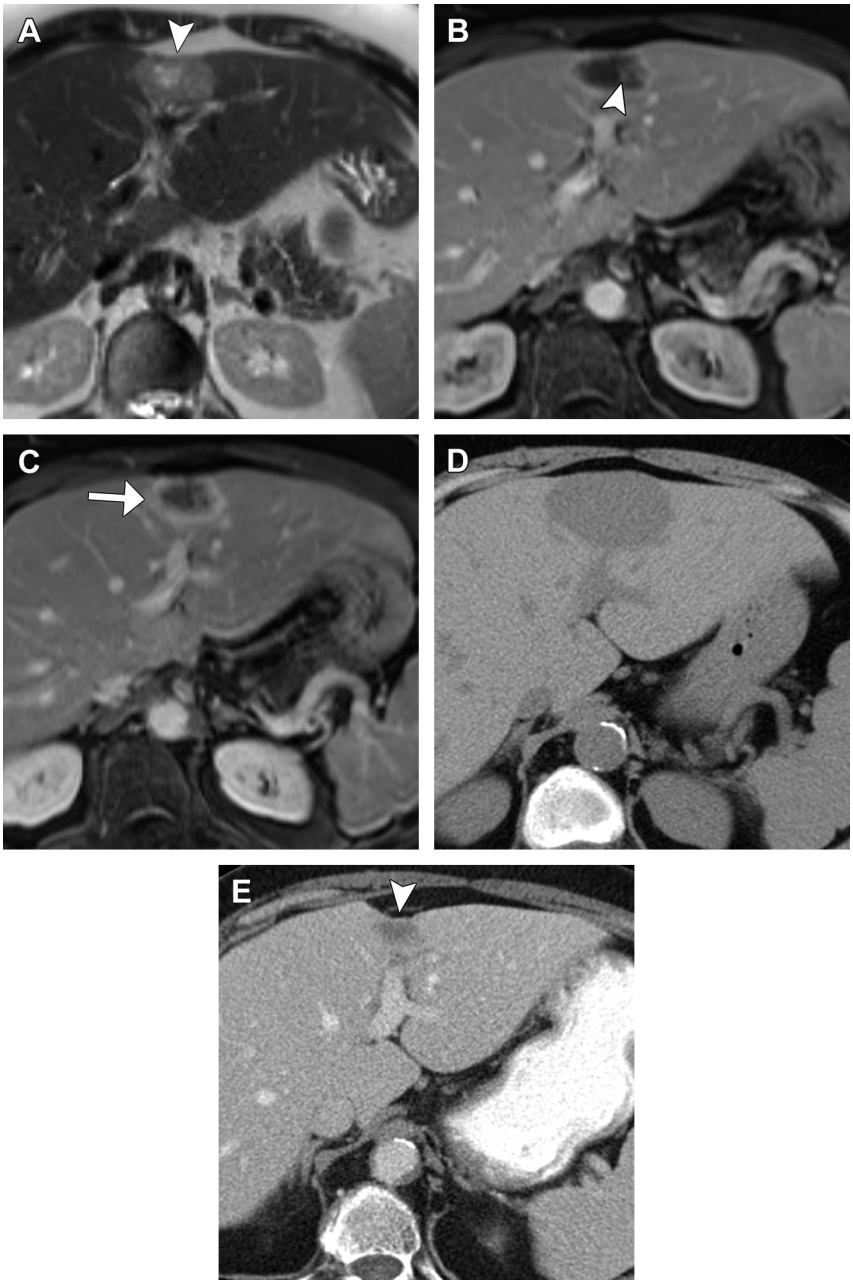

Fig. 4. Sclerosing hemangioma (*A*) Heterogeneous, mildly T2 hyperintense mass with overlying capsular retraction (*arrowhead*). (*B*) Portal venous phase image demonstrates a continuous rim of enhancement with some internal nodular foci of enhancement (*arrowhead*). (*C*) Equilibrium phase image shows progressively thick rim of peripheral enhancement (*arrow*). Biopsy performed at this time was consistent with a hemangioma. (*D*) Noncontrast CT image from an outside institution 2 years prior shows that the mass was previously larger. (*E*) One year later, it continued to decrease in size with progressive capsular retraction (*arrowhead*).

related to compression of adjacent liver parenchyma, perilesional vessels, or an inflammatory reaction.[29,35] Rare instances of fat accumulation within FNH have been reported in the literature, a finding usually suggestive of HCA or hepatocellular carcinoma (HCC).[30,36] Fat within FNH may be more commonly seen with diffuse hepatic steatosis but the lesion will often have other features typical of FNH. FNH is most commonly solitary; these atypical features have been more

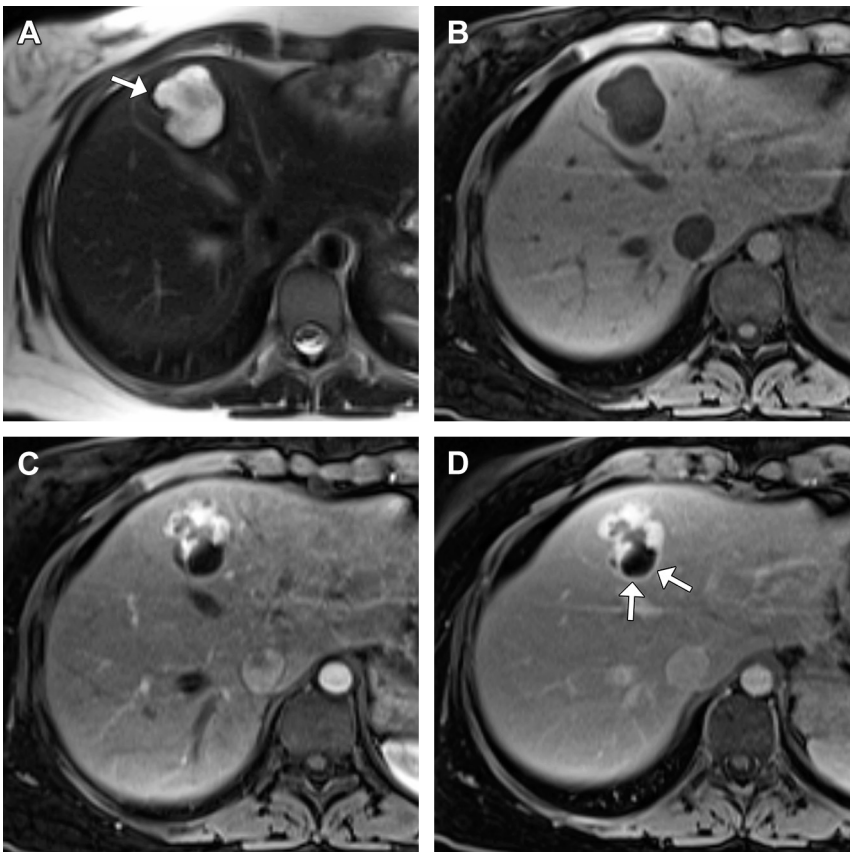

Fig. 5. Potential pitfall: solitary sarcoma metastasis mimicking hepatic hemangioma. (*A*) Slightly lobulated T2 hyperintense mass in segment 4a has circumscribed margins (*arrow*). (*B*) It is uniformly T1 hypointense. (*C*) Irregular peripheral nodular enhancement is seen during arterial phase. (*D*) Equilibrium phase shows no progressive filling; however, note the thin continuous rim of enhancement along its posterior wall (*arrows*). This mass grew on short-term follow-up imaging. Biopsy confirmed a metastasis in this patient with a history of rhabdomyosarcoma.

commonly reported in the setting of multiple FNH lesions.[35]

Small FNH lesions often lack a visible central scar and this should not be misconstrued as an atypical feature. In one study, 42 (80%) of 49 FNH lesions 3 cm in size or smaller lacked a central scar.[37] Conversely, central scars may be seen in other lesions, including fibrolamellar carcinoma and HCC.[38] One must always relate the imaging findings with the clinical context. By definition, a diagnosis of FNH should not be made in a cirrhotic liver.[39] Because fibrolamellar carcinoma also occurs in young adults without underlying liver disease, other features must be used to distinguish it from FNH. The central scar of fibrolamellar carcinoma is usually hypointense on all sequences and does not enhance, owing to collagen and/or coarse calcification.[40] Rarely, it appears T2 hyperintense with delayed enhancement due to increased vascularity, mimicking the central scar of FNH.[40,41] Confounding the issue, the central scar in FNH can show atypical features, such as low T2 signal intensity or only mild enhancement during the equilibrium phase.[29,35] Clues useful for distinguishing fibrolamellar carcinoma from FNH include large size (>10 cm), tumor heterogeneity, large scar (width >2 cm), calcification, invasion of adjacent vessels, lymphadenopathy, and extrahepatic metastases.[38] In addition, fibrolamellar carcinoma is relatively rare compared with FNH.

Due to overlapping patient populations and imaging features, a common diagnostic challenge is to distinguish atypical FNH from HCA, an important distinction that may alter patient management. The hepatocyte-specific contrast agent gadoxetate disodium can be useful in such cases. FNH contains densely packed functioning hepatocytes and abnormal blind-ending bile ductules, resulting in contrast retention and delayed biliary excretion. FNH often shows vivid enhancement

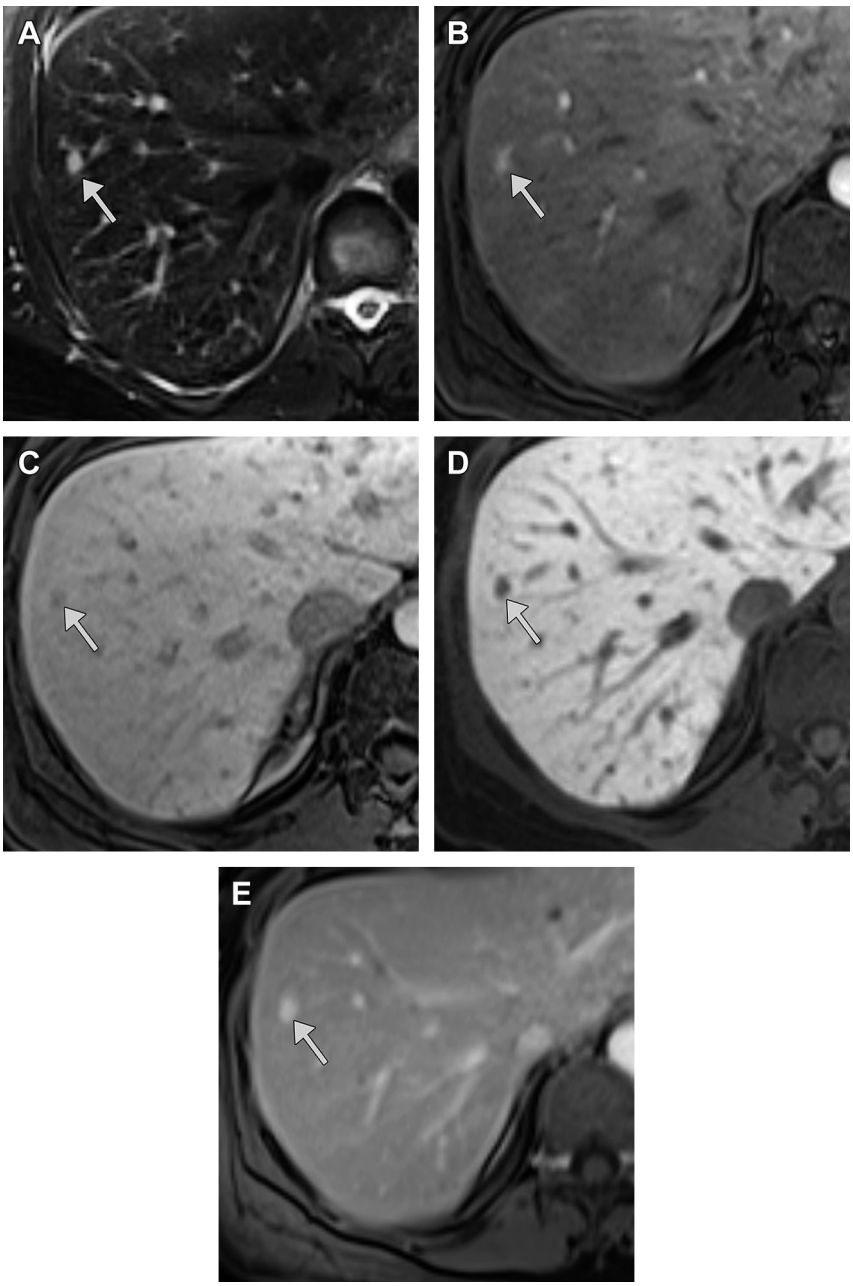

Fig. 6. Potential pitfall: pseudowashout of a flash-filling hemangioma with gadoxetate disodium-enhanced MR imaging. (*A*) T2-weighted fat-suppressed image shows a small circumscribed T2 hyperintense lesion (*arrow*). (*B*) Gadoxetate disodium–enhanced MR imaging reveals uniform arterial hyperenhancement (*arrow*). (*C*) The lesion becomes hypointense relative to the increasingly bright liver parenchyma during equilibrium phase, simulating washout (*arrow*). (*D*) It is uniformly hypointense to liver on hepatocyte phase (*arrow*), as expected for a hemangioma. (*E*) Same patient examined with an extracellular contrast agent displays the more familiar appearance of hemangioma retaining contrast on delayed images (*arrow*).

on delayed hepatocyte-phase images, although the degree can vary.[2,4] In a study by van Kessel and colleagues,[42] 19 (73%) of 26 cases of FNH were hyperintense or at least isointense to liver on delayed images, 23% were predominately hypointense with a hyperintense rim, and only 1 case was hypointense without an enhancing rim. The central scar does not typically retain contrast

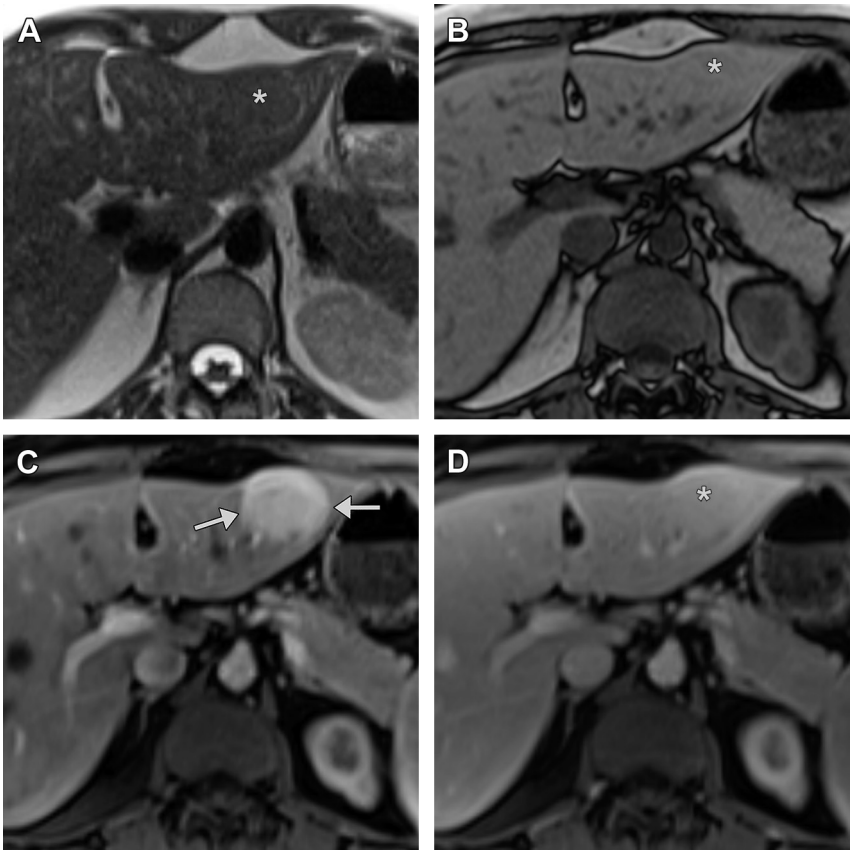

Fig. 7. FNH as "stealth" lesion. (*A*) There is a slight contour bulge of the lateral left hepatic lobe due to an underlying T2 isointense mass (*asterisk*). (*B*) The mass is isointense to liver on opposed-phase T1-weighted imaging (*asterisk*), unlike a fat-containing lesion. (*C*) It demonstrates uniform arterial hyperenhancement (*arrows*). (*D*) It then fades to become nearly isointense to liver during portal venous phase (*asterisk*).

on delayed images using gadoxetate disodium, and together with radiating fibrous septae, it may result in a characteristic spoke-wheel appearance.[4,43] Conversely, HCAs are usually hypointense to liver on hepatocyte phase images because, although they have functioning hepatocytes, they lack bile ductules.[37] However, HCAs can occasionally appear isointense or even hyperintense to liver with the underlying mechanism of transport poorly understood.[4]

Hepatocellular Adenoma

HCA is a less common benign primary neoplasm of the liver. Though most often encountered in women of childbearing age taking oral contraceptives, it can occur in other women as well as men. In recent years, HCA has been categorized into 3 distinct subtypes based on genetic and pathologic features: (1) inflammatory, (2) hepatocyte nuclear factor 1-alpha (HNF-1α) inactivated, and (3) β-catenin-activated lesions. Some exhibit both β-catenin-activation and inflammatory features.[44] Unclassified HCAs are a small group that lack specific morphologic or immunophenotypical features.[45]

Inflammatory HCA is the most common subtype (40%–50%) and includes lesions formerly known as "telangiectatic" FNH or HCA. It occurs most frequently in young women on oral contraceptives and in obese patients. Histopathology reveals intense polymorphous inflammatory infiltrates, marked sinusoidal dilatation, and abnormal thick-walled arteries.[46] HNF-1α–inactivated HCA is the second most common subtype (30%–35%), resulting from biallelic inactivation of the HNF-1α tumor suppressor gene. This also inactivates liver fatty acid–binding protein, leading to intralesional fat deposition. This subtype occurs exclusively in women, most of whom (>90%) take oral contraceptives; some are also associated with maturity-onset diabetes of the young (MODY) type 3 and familial hepatic adenomatosis.[46] The β-catenin mutated HCA subtype (10%–15%) occurs with sustained activation of the β-catenin

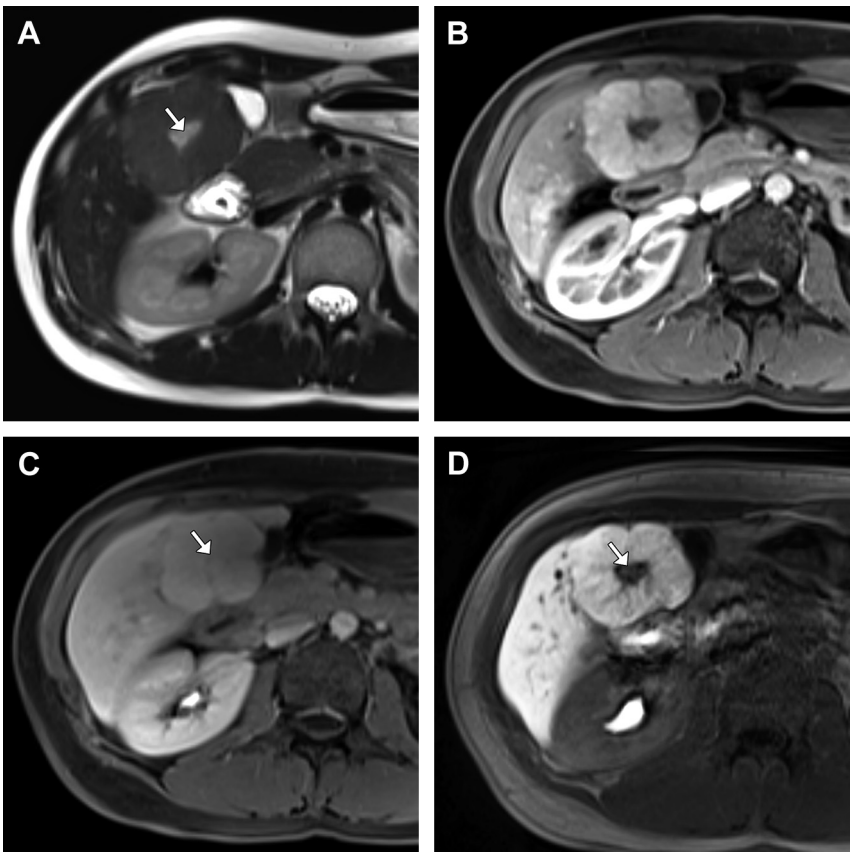

Fig. 8. FNH with central scar; gadoxetate disodium–enhanced MR imaging. (*A*) Slightly T2 hyperintense mass has a focal T2 bright central scar (*arrow*). (*B*) The mass demonstrates uniform arterial hyperenhancement. (*C*) There is delayed enhancement of the central scar during equilibrium phase (*arrow*). (*D*) On 20-minute delayed hepatocyte phase images, the mass retains contrast while its central scar does not (*arrow*).

gene, resulting in uncontrolled hepatocyte formation; it occurs more frequently in men and is associated with anabolic steroid use, glycogen storage disease, and familial adenomatosis polyposis.[46]

HCAs are reported to be solitary in most cases (70%–80%), but it is not uncommon for a patient to have 2 or 3 lesions at imaging.[47] Some have found that HCAs are more often multiple in the setting of hepatic steatosis.[48] Presence of more than 10 lesions is rare, originally defined as "liver adenomatosis" by Flejou and colleagues[49] in 1985 as a distinct entity occurring in men and women without risk factors for HCA. It had been suggested that the lesions in adenomatosis are not steroid dependent and are more likely to lead to impaired liver function, hemorrhage, and possibly malignant degeneration.[50] However, more recent evidence suggests adenomatosis is not a specific entity, as once thought, and that lesion size and subtype, not overall number, are important to consider for possible complications.[51]

HCAs are usually well defined, sometimes with a capsule (17%–30%), and can range in size from smaller than 1 cm to larger than 15 cm.[47,52,53] Most patients are asymptomatic at the time of discovery, but some present with abdominal pain, hemorrhage, abnormal liver function tests, or seldom with a palpable mass.[51] The overall rate of hemorrhage is 20% to 25%; larger size (>5 cm) and subcapsular location are risk factors for rupture and bleeding.[46,54] Of the different subtypes, inflammatory HCAs may be more prone to bleed owing to sinusoidal dilatation, peliotic areas, and abnormal arteries.[46]

According to a meta-analysis by Stoot and colleagues,[55] the rate of malignant transformation of HCA to HCC is 4.2%; this occurs more commonly in lesions larger than 5 cm and in men.[53,54] The β-catenin-activated subtype carries the highest risk of malignant transformation; however, some inflammatory HCAs regardless of β-catenin status may also develop HCC.[45] HNF-1α–inactivated HCAs carry the lowest risk of malignant

transformation.[45] Thus, recognition of subtype may be relevant with regard to how patients are managed.

As a group, HCA has a variable appearance at imaging; yet, investigators have shown that specific MR imaging patterns may allow for pathologic subtype characterization. Diffuse intralesional fat deposition on chemical shift imaging is characteristic of HNF-1α–inactivated HCA; this finding alone is 86.7% sensitive and 100% specific for HCA subtype characterization (**Fig. 9**).[44] Intralesional fat is seen much less often with inflammatory HCAs, but when it does occur it is usually focal or patchy and heterogeneous rather than uniformly diffuse.[44,45,56] Owing to typical findings of sinusoidal dilatation at histopathology, distinguishing features of inflammatory HCAs include (1) marked T2 hyperintensity, especially in the periphery of the lesion, and (2) strong arterial phase enhancement that persists on more delayed images. Together, these 2 findings are 85.2% sensitive and 87.5% specific for diagnosis (**Fig. 10**).[44] van Aalten and colleagues[56] observed a characteristic "atoll sign" in nearly half (43%) of inflammatory HCAs in their series but not with other subtypes. This refers to a lesion with a peripheral ringlike band of T2 hyperintense signal and a central portion that is isointense to the liver, thus resembling a coral atoll (**Fig. 11**). van Aalten and colleagues[56] suggested that findings of vaguely defined scars or poorly defined T2 hyperintense areas within a lesion might be related to β-catenin-activation (**Fig. 12**), but larger sample sizes are needed to confirm this association. For now, biopsy remains the best option for diagnosing this subtype at greatest risk for malignant transformation.

Imaging features of HCA may overlap with other lesions. In young, otherwise healthy patients, the differential diagnosis commonly includes FNH. Lesion heterogeneity in this population is more suggestive of HCA, particularly if there is variable T1 signal intensity related to hemorrhage or fat content.[52,57] Central scars characteristic of FNH are rarely seen in HCA.[53] Intralesional fat is much more commonly seen in HCA. Nonetheless, it may be difficult to distinguish some HCAs from atypical FNHs, and gadoxetate disodium–enhanced MR imaging may prove helpful in this setting. Distinguishing HCA from HCC is of even greater importance. Both may contain intralesional fat (up to 40% of HCC).[52] Both typically show arterial hyperenhancement. Occasionally, HCA will demonstrate washout or presence of a capsule, other shared features with HCC. Clinical history, including patient demographics and any risk factors for HCC, as well as the background appearance of the liver, including cirrhotic morphology, should provide clues to the correct diagnosis.

Proposed management strategies for HCA rely on cross-sectional imaging for diagnosis and subtype characterization, as well as clinical history and lesion size to determine the need for biopsy or surgical resection. For simplification, HCAs can be initially characterized at MR imaging as (1) diffusely steatotic or (2) either heterogeneous or nonsteatotic. If the patient is taking oral contraceptives or steroids, repeat imaging is recommended 3 to 6 months after discontinuation.[46] Stable and regressing HCAs may be monitored with continued follow-up. Growing lesions warrant further evaluation based on patient sex and lesion size. Surgical resection is advocated for large HCAs (>5 cm) and any HCAs found in men or patients with glycogen storage disease due to an association with β-catenin-activated subtype and increased HCC risk.[46] Females with small (<5 cm) heterogeneous HCAs may warrant percutaneous biopsy to search for β-catenin mutation.[46] Females with small (<5 cm) diffusely steatotic HCAs are at low risk for malignancy, but may benefit from genetic counseling regarding family history of HCA, adenomatosis, and/or MODY type 3.[46,51]

PYOGENIC LIVER ABSCESS

Pyogenic liver abscesses (PLAs) are localized collections of pus resulting from bacterial infection with destruction of the liver parenchyma and stroma.[58,59] PLAs account for 80% of liver abscesses of all varieties in the United States and Western countries.[60] They may develop as a result of ascending cholangitis (due to benign or malignant biliary obstruction or complication of biliary procedures), hematogenous spread of gastrointestinal infection via the portal vein, diffuse septicemia via the hepatic artery, intrahepatic rupture of cholecystitis, or superinfection of necrotic tissue.[58,61]

With advances in antimicrobial therapy and surgical and/or medical management, biliary tract pathology has surpassed portal seeding from appendicitis and diverticulitis as the most common source of PLA.[62,63] Meddings and colleagues[64] observed the incidence of PLA (3.6 per 100,000) in the United States to be rising and attributed this to an aging population and growing prevalence of hepatobiliary disease, biliary intervention, diabetes, and liver transplantation, all known risk factors for PLA. Diabetes is also implicated in many of the so-called cryptogenic cases of PLAs.[65]

PLAs resulting from hematogenous spread of infection usually manifest as one or a few

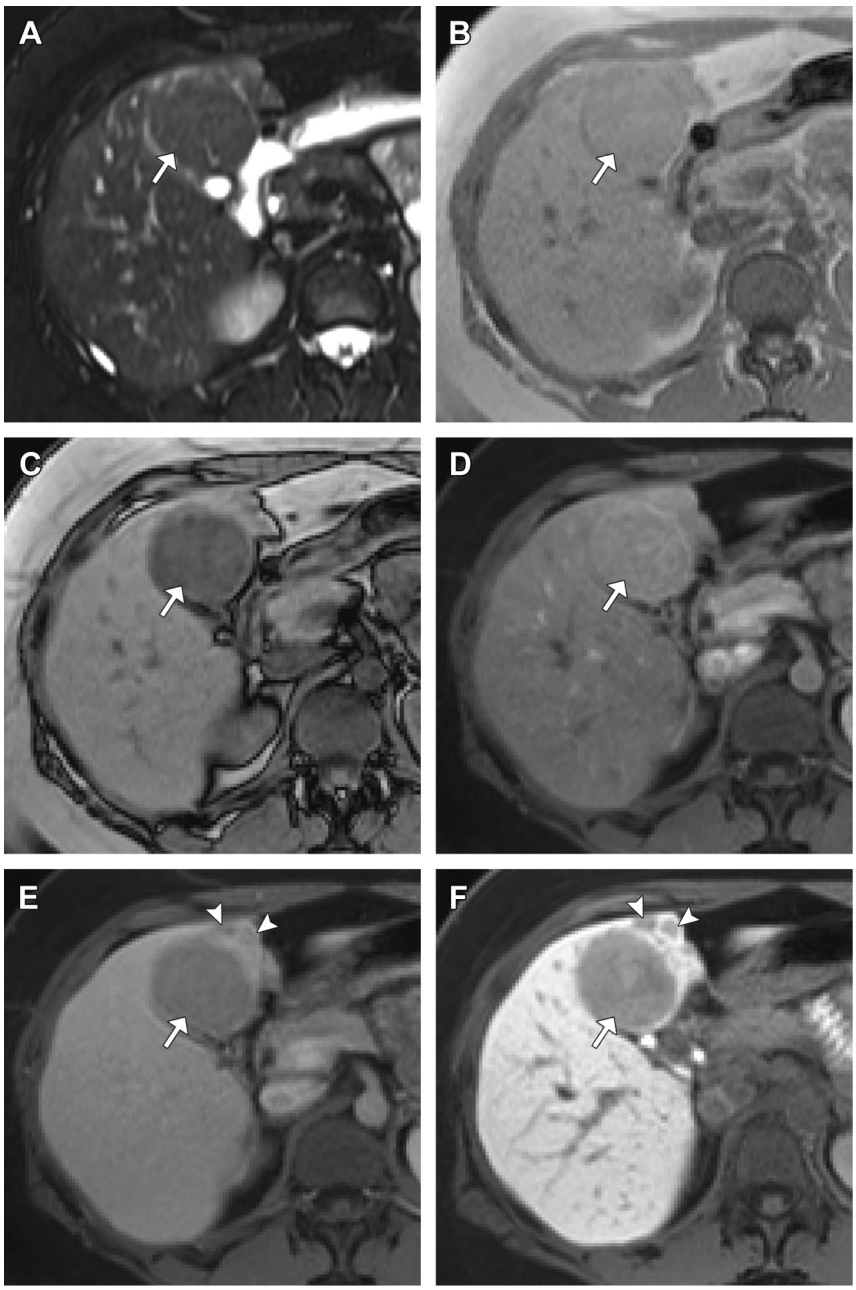

Fig. 9. HCA (HNF-1α–inactivated or steatotic subtype); gadoxetate disodium–enhanced MR imaging. (*A*) T2-weighted fat-suppressed image demonstrates a uniformly isointense hepatic mass (*arrow*). (*B*) The mass is isointense to liver on in-phase T1-weighted imaging (*arrow*). (*C*) Diffuse signal dropout of the mass on opposed-phase T1-weighted imaging indicates intracellular fat (*arrow*). (*D*) The mass uniformly enhances to a slightly greater degree than adjacent liver during arterial phase (*arrow*). (*E*) The mass becomes hypointense relative to liver during portal venous phase ("washout") (*arrow*); subtle small adjacent lesions also become apparent (*arrowheads*). (*F*) The dominant mass (*arrow*) and small adjacent lesions (*arrowheads*) all remain hypointense to liver during hepatocyte phase, with the small lesions best seen on this series. Multiple HCAs were confirmed at resection.

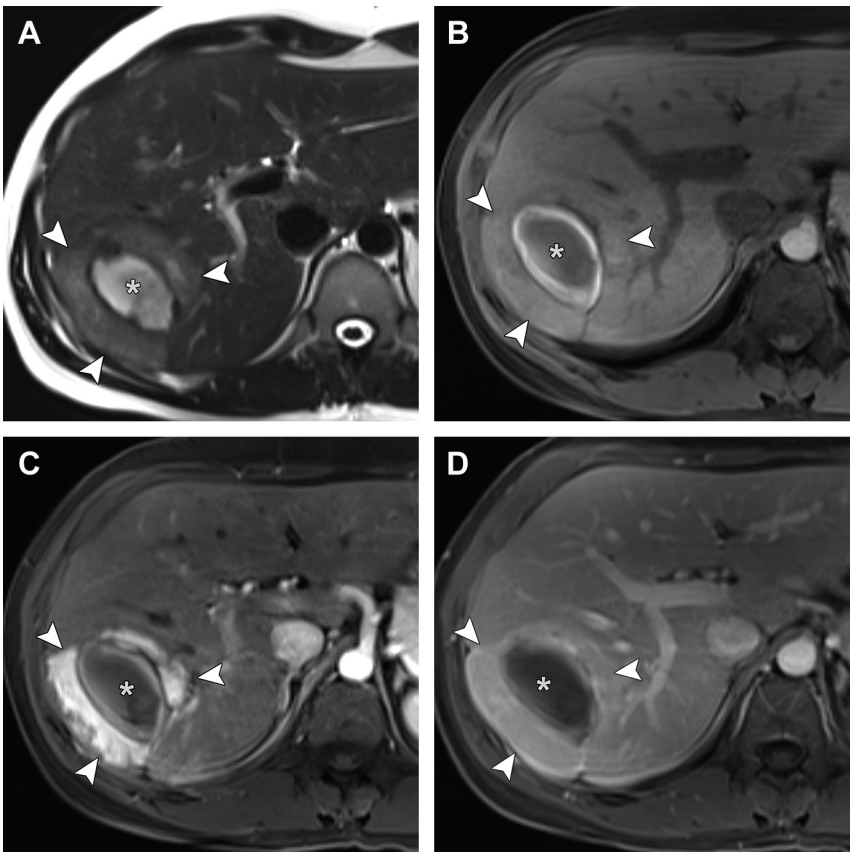

Fig. 10. HCA complicated by hemorrhage (inflammatory subtype). (*A*) Slightly T2 hyperintense mass (*arrowheads*) in the posterior right lobe contains a central ovoid region of bright signal surrounded by a thin T2 hypointense rim (*asterisk*). (*B*) The mass itself is isointense to liver on T1-weighted fat-suppressed images (*arrowheads*), whereas the central region is partially T1 hyperintense compatible with blood products (*asterisk*). (*C*, *D*) Postcontrast images demonstrate strong arterial hyperenhancement of the mass (*arrowheads*) that persists on delayed images without washout. The central region does not enhance, in keeping with hemorrhage (*asterisk*). Surgical pathology revealed inflammatory HCA, which is suggested by its T2 signal intensity and enhancement pattern; inflammatory HCA is the subtype most prone to hemorrhage.

large lesions, with preference for the right lobe due to its size and propensity to receive most of the portal blood flow.[58,66] PLAs of biliary origin tend to be greater in number and smaller in size[58]; those smaller than 2 cm may be classified as microabscesses.[61] Solitary abscesses are more likely than multiple abscesses to be polymicrobial.[63] Common causative organisms are *Streptococcus* species, *Escherichia coli*, and *Klebsiella*, with *Klebsiella* accounting for the highest percentage of cases in large recent Asian case studies.[60,63,64,67,68]

Most patients have fevers at the time of presentation, as many as 99% in one case series by Wong and colleagues.[67] Patients also commonly experience chills and right upper quadrant pain.[60,65] However, the presenting symptoms of PLA can be highly variable. Clinically occult or "cold" abscesses manifest with nonspecific symptoms, such as weight loss or vague abdominal pain.[61]

PLAs can have a variable appearance at MR imaging, but are generally sharply marginated and T2 hyperintense and T1 hypointense. Microabscesses are more difficult to appreciate on precontrast T1-weighted images but become more conspicuous after contrast due to central nonenhancement.[58] Intense early wall enhancement is characteristic, usually between 2 and 5 mm in thickness and relatively uniform (**Fig. 13**).[69] This wall enhancement persists on delayed images, with little to no perceptible change in thickness.[69] Internal septations are occasionally seen (**Fig. 14**). A focal cluster of microabscesses separated by enhancing septae suggests the early stage of coalescence into a larger abscess cavity.[58] This

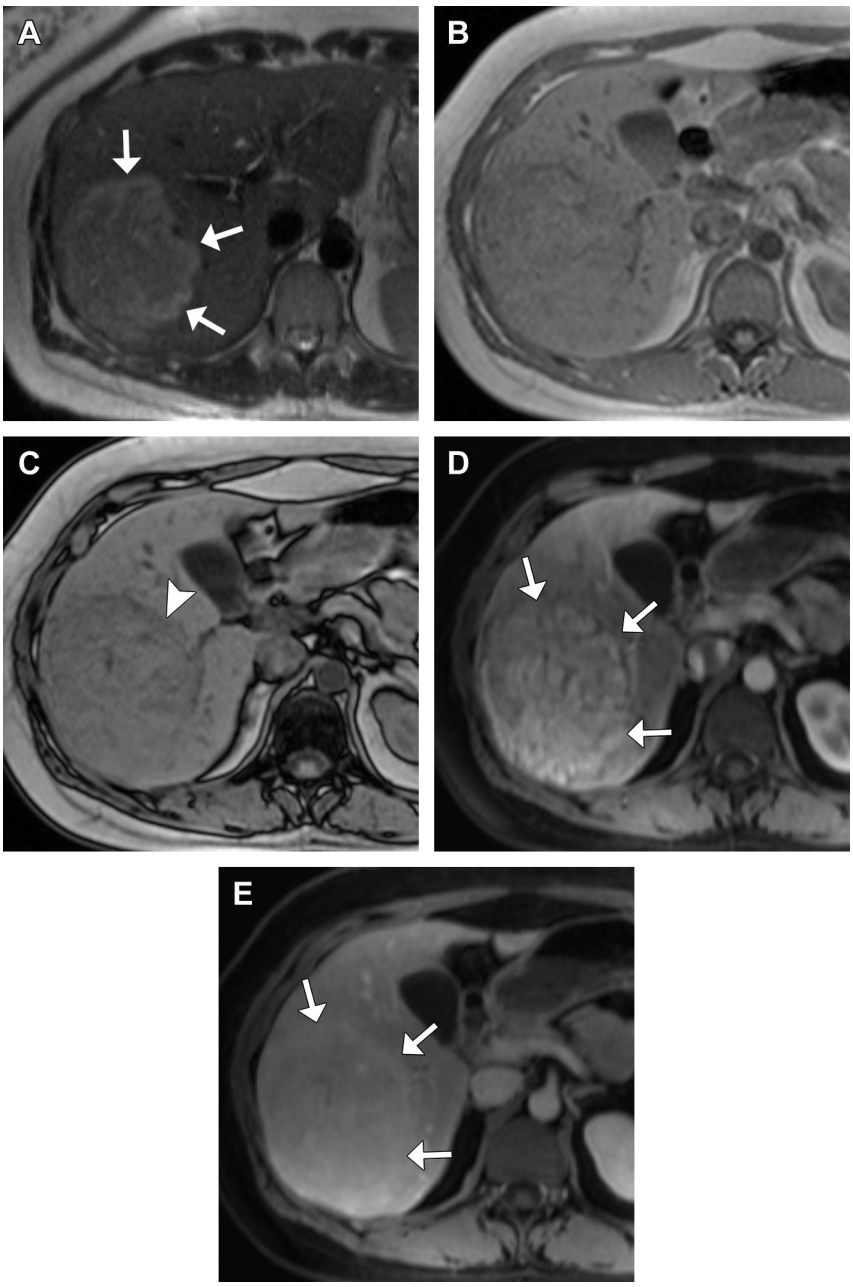

Fig. 11. HCA (inflammatory subtype): "atoll sign." (*A*) Large right hepatic mass exhibits a peripheral ringlike band of T2 hyperintense signal (*arrows*) and less pronounced mildly T2 hyperintense signal centrally, with overall appearance likened to a coral atoll. (*B*) The mass is nearly isointense to liver on in-phase T1-weighted imaging. (*C*) There is subtle signal loss on opposed-phase T1-weighted imaging suggesting intracellular fat (*arrowhead*), although not as pronounced or diffuse as described with HNF-1α–inactivated subtype. (*D*, *E*) Postcontrast images demonstrate arterial hyperenhancement that persists on delayed imaging (*arrows*). Inflammatory HCA was found at resection.

so-called "cluster sign" favors a diagnosis of PLA over other types of liver abscesses.[70]

Perilesional edema manifested by mild increased T2 signal and/or perilesional enhancement differences is not uncommon, especially with larger abscesses. Patterns include (1) adjacent wedge-shaped transient arterial hyperenhancement alone or (2) adjacent wedge-shaped or circumferential surrounding edema with associated hyperenhancement during arterial and

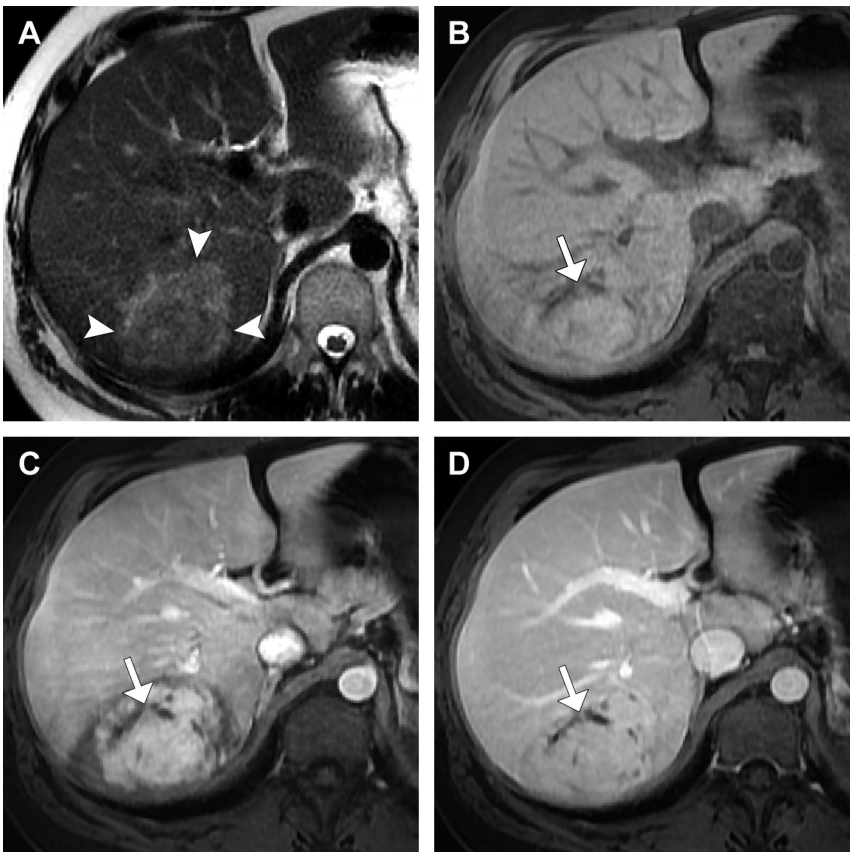

Fig. 12. HCA (β-catenin-activated subtype) in a 31-year-old male. (*A*) Heterogeneous, mildly T2 hyperintense mass in the posterior right lobe has a peripheral band of mildly T2 hyperintense signal (*arrowheads*). (*B*) Precontrast fat-suppressed T1-weighted image demonstrates an eccentric poorly defined T1 hypointense scar (*arrow*). (*C*) The mass exhibits heterogeneous arterial hyperenhancement and slightly more uniform enhancement during portal venous phase (*D*) with exception of the nonenhancing eccentric scar (*arrows*). HCA with β-catenin mutation was found at resection. This subtype occurs more frequently in men. It has been suggested that vaguely defined scars or poorly defined T2 hyperintense areas within a lesion might relate to β-catenin activation, but this is not definitive and biopsy remains the best option for diagnosing this subtype.

delayed phases.[69] Perilesional edema also has been described as highly suggestive of abscess formation at CT.[71] Proposed etiologies include adjacent sinusoidal dilatation or inflammatory response.[58]

DWI is very helpful in making the diagnosis of PLA. Due to the high viscosity and cellularity of pus, abscess cavities demonstrate restricted diffusion (see **Figs. 13** and **14**).[59] This allows for quick differentiation of PLAs from benign cysts that lack restricted diffusion. Some investigators also have suggested that DWI can potentially help differentiate PLAs from certain cystic or necrotic primary or metastatic liver neoplasms, as abscess cavities may demonstrate overall greater restricted diffusion (lower ADC values).[7,59]

Prompt diagnosis and treatment of PLA is necessary for a good outcome. Identifying a potential source, such as diverticulitis, biliary disease, or appendicitis, is critical and may require additional imaging. Broad-spectrum antibiotics should be initiated and subsequently modified once sensitivities become available. Antibiotics alone can be effective for some patients with small (<3 cm) abscesses[62]; however, most PLAs require drainage and/or treatment of underlying biliary obstruction if present.[58] Image-guided percutaneous catheter drainage has replaced surgical intervention as the most common approach.[62,72]

HEPATIC CYSTS

Simple hepatic cysts are common benign liver lesions that are typically incidentally discovered. They are usually round or ovoid with smooth margins and range in size from a few millimeters to

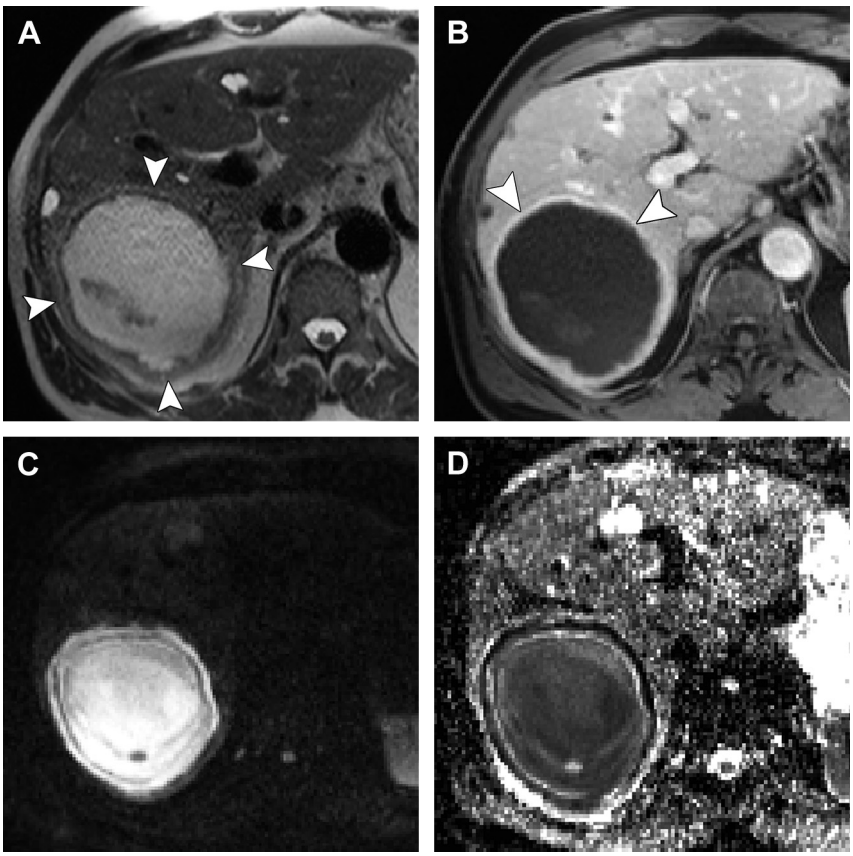

Fig. 13. Pyogenic liver abscess. (*A*) Large rounded predominately T2 hyperintense mass in the posterior right lobe has a rim of mild increased T2 signal that may in part relate to surrounding edema (*arrowheads*). (*B*) Postcontrast images show relatively uniform wall enhancement (*arrowheads*). (*C*) Contents are markedly hyperintense on the high b-value (800 s/mm^2) diffusion-weighted image. (*D*) Pronounced low signal on the corresponding ADC map indicates restricted diffusion, typical of abscess.

several centimeters. On MR imaging, simple cysts are markedly T2 hyperintense and T1 hypointense (isointense to fluid), have very thin or imperceptible walls, and do not enhance following contrast.[73,74]

CILIATED HEPATIC FOREGUT CYST

Ciliated hepatic foregut cyst (CHFC), a term first used by Wheeler and Edmondson in 1984,[75] is an uncommon solitary benign hepatic cyst that appears histologically similar to bronchogenic and esophageal duplication cysts. It is thought to arise due to abnormal budding of the embryologic foregut. Characteristically, it is lined by a pseudostratified, ciliated, mucin-secreting, columnar epithelium, with bands of smooth muscle in the cyst wall and an outer fibrous capsule.[75]

CHFCs are likely underdiagnosed but important to not confuse with malignancy. Most often, a CHFC is found within or in close proximity to the medial left hepatic lobe (segment 4).[76] Subcapsular location is also characteristic[77]; in some cases, the cyst wall extends slightly beyond the contour of the liver.[78] It is typically unilocular with an average size of 3.6 cm (range of 1.1–13.0 cm).[76] Most cases are diagnosed in the fifth or sixth decade, with a slight male predominance (1.1:1.0 ratio).[76,79]

The true prevalence of CHFC is difficult to establish, as most are asymptomatic and discovered incidentally.[80] Some believe they do not cause symptoms unless they become infected or large enough to compress adjacent organs.[78] Rare cases of very large CHFCs resulting in obstructive jaundice[80,81] and portal hypertension[82] due to mass-effect on the biliary tree and portal vein, respectively, have been reported. Malignant transformation is another rare complication; at least 4 cases of squamous cell carcinoma arising in CHFC have been reported in the literature.[83–86]

The diagnosis may be difficult at CT, as the fluid may be complicated and of greater density than

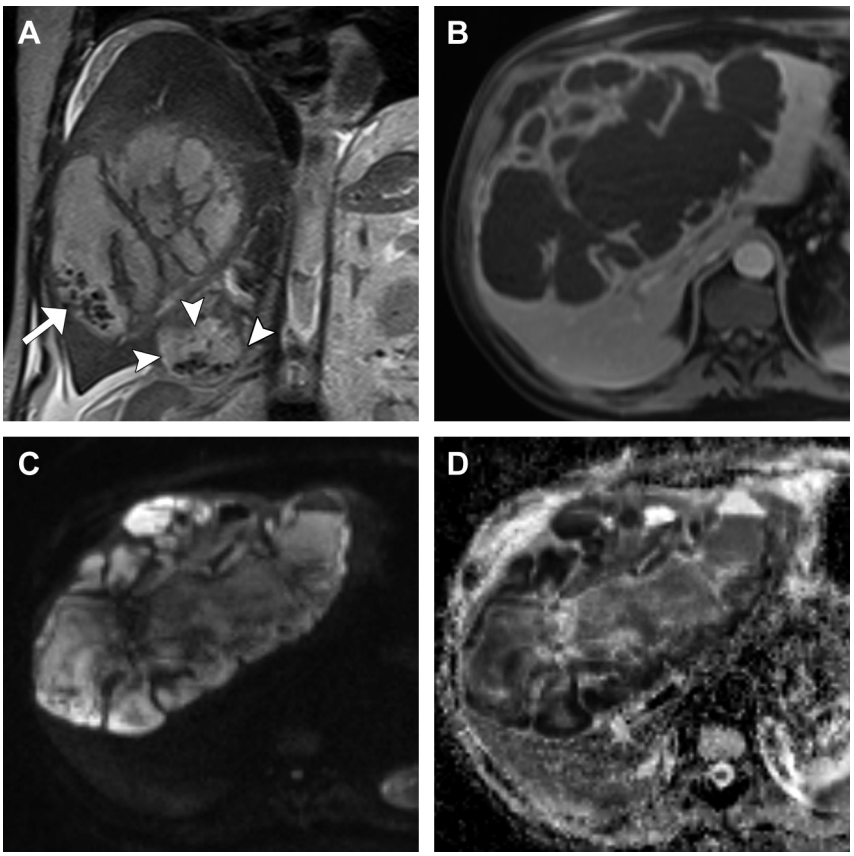

Fig. 14. Large pyogenic liver abscess due to intrahepatic rupture of cholecystitis. (*A*) Coronal T2-weighted image shows a large multiloculated T2 hyperintense hepatic mass containing several tiny spilled gallstones (*arrow*). Gallstones are also seen in the adjacent gallbladder (*arrowheads*). (*B*) Postcontrast image during equilibrium phase shows diffuse enhancement of its outer wall and several internal septae. (*C*) The mass exhibits restricted diffusion, with bright signal on the high b-value (800 s/mm^2) diffusion-weighted image and low signal on the corresponding ADC map (*D*).

simple fluid, potentially mimicking a solid and/or hypovascular or necrotic mass.[77,87] MR imaging better demonstrates their cystic nature and proteinaceous fluid content (**Fig. 15**). They are well-defined, T2 hyperintense, and mostly unilocular lesions. Variable signal intensity on T1-weighted images, ranging from hypointense to hyperintense signal, reflects differences in protein concentration.[78] Rarely, they may be associated with a fluid-fluid level.[79] Contrast-enhanced images easily confirm their cystic nature by demonstrating only thin wall enhancement.[78] Primary differential considerations include simple or complicated (infected or hemorrhagic) cysts and biliary cystadenomas. CHFCs should be diagnosed based on their classic subcapsular location in the medial segment of the left hepatic lobe.

CHFCs generally have a benign course. Surgical excision is recommended for symptomatic and/or large lesions producing mass-effect.[82,84] Because case reports of malignant transformation with poor outcomes have been described, some have recommended surgical excision or enucleation of CHFCs regardless of size.[76] Current data may be limited by small sample sizes. Regardless, careful attention can be made at imaging for any irregular wall thickness or solid component that might suggest the rare development of carcinoma.

BILE DUCT HAMARTOMAS

Bile duct hamartomas (BDH), also known as biliary hamartomas and von Meyenburg complexes, are benign liver lesions that result from ductal plate malformations involving the small interlobular bile ducts.[88] They consist of focally disordered collections of bile ducts surrounded by abundant fibrous stroma[89] and are considered part of a spectrum of fibropolycystic liver disease that also includes

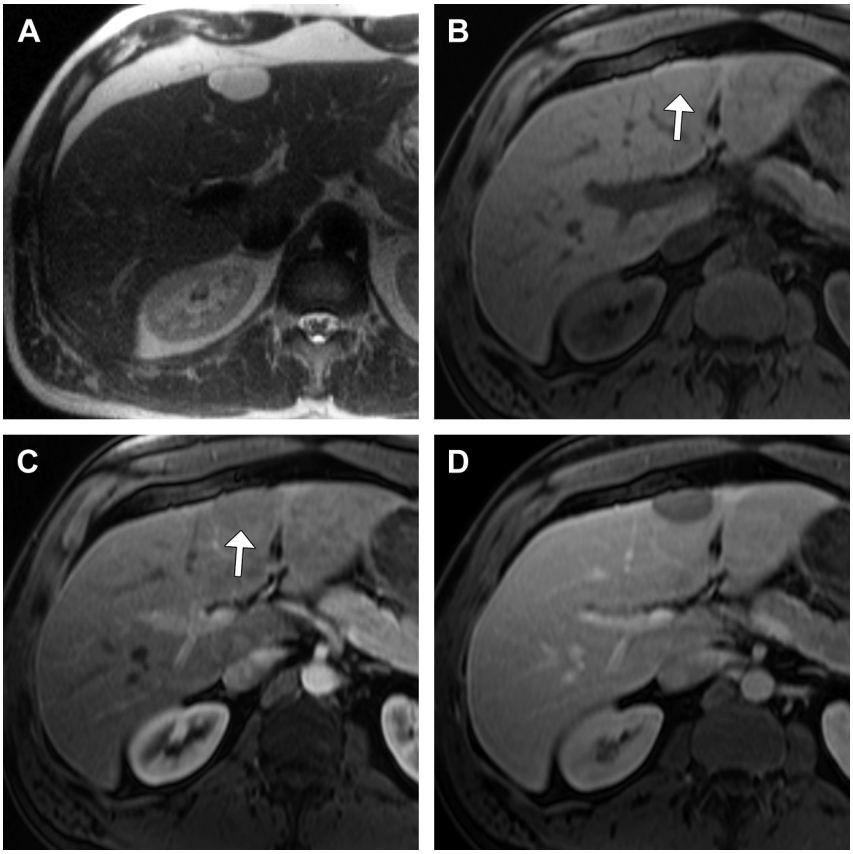

Fig. 15. Ciliated hepatic foregut cyst. (*A*) Typical subcapsular T2 hyperintense cystic lesion in segment 4 extends slightly beyond the contour of the liver. (*B*) On precontrast fat-suppressed T1-weighted imaging, this appears isointense to liver due to proteinaceous fluid content (*arrow*). (*C*) The lesion remains nearly isointense to adjacent liver parenchyma during arterial phase (*arrow*). (*D*) It becomes hypointense to liver during the portal venous phase but should not be mistaken for a solid enhancing lesion with "washout."

congenital hepatic fibrosis, autosomal dominant polycystic liver disease, and Caroli disease.[90]

BDHs can vary in number from as few as 1 or 2 small (≤10 mm) cystic liver lesions to numerous scattered small lesions of near uniform or varying size (**Fig. 16**).[89] Initial case reports warned of potential confusion with metastases, especially in patients with known extrahepatic malignancy[91,92]; however, MR imaging readily distinguishes BDHs from solid lesions.[90] They are well-defined T2 hyperintense cystic lesions that lack communication with the biliary tree and may exhibit lobulated

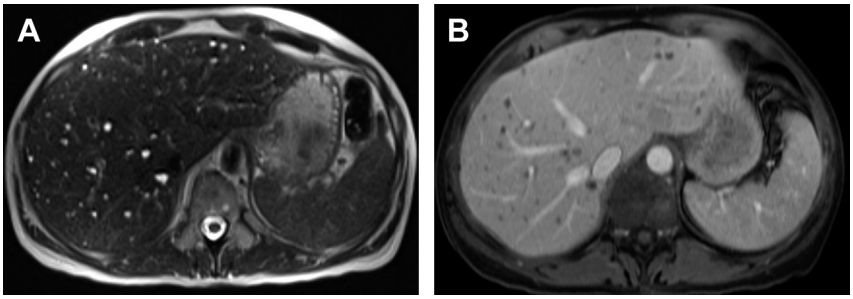

Fig. 16. Multiple bile duct hamartomas. (*A*) Numerous subcentimeter T2 hyperintense cystic foci are scattered throughout the liver. (*B*) The lesions appear hypointense to liver on postcontrast images and should not to be mistaken for hypoenhancing solid lesions or metastases.

margins, thin septations, and a characteristic thin rim of enhancement related to adjacent compressed liver parenchyma and inflammation (**Fig. 17**).[90,92] Identification of a 1-mm to 2-mm "mural nodule" owing to conjunctive septae within at least one lesion has been proposed to increase diagnostic specificity of BDH.[88] Overall, these cyst wall features may help in the differentiation from simple cysts, although this distinction is usually not needed, as most BDHs are of no clinical significance.[90] Lack of restricted diffusion helps distinguish them from microabscesses.

More recently, Martin and colleagues[90] described less common large cystic and complicated variants they collectively named "giant BDH." This term applies to lesions larger than 2 cm, although they can be much larger (>10 cm) and develop complications, such as hemorrhage and right upper quadrant pain.[90] A clue to diagnosis is that they coexist with smaller typical BDHs and have less internal complexity than biliary cystadenomas (BCAs).

BILIARY CYSTADENOMA

BCA is a rare cystic neoplasm that is generally found in middle-aged women but can occur at any age and occasionally in men. It is histologically similar to mucinous cystic neoplasm of the pancreas.[93,94] Many believe that all BCAs are premalignant. Lesions are subdivided at pathology based on the presence or absence of ovarian stroma, found only in women and considered a favorable prognostic indicator.[93] Typical gross pathology features include a characteristic multilocular appearance[95] and presence of a fibrous capsule.[93]

Most BCAs are intrahepatic (85%), but they also may arise from the common duct or rarely the gallbladder.[93] They are usually large lesions, with a mean size of 12 cm in one larger series (ranging from 3 to 40 cm).[93] Often slow growing, they may present with nonspecific symptoms, such as abdominal pain.[93,95,96] Some patients present with jaundice from associated biliary

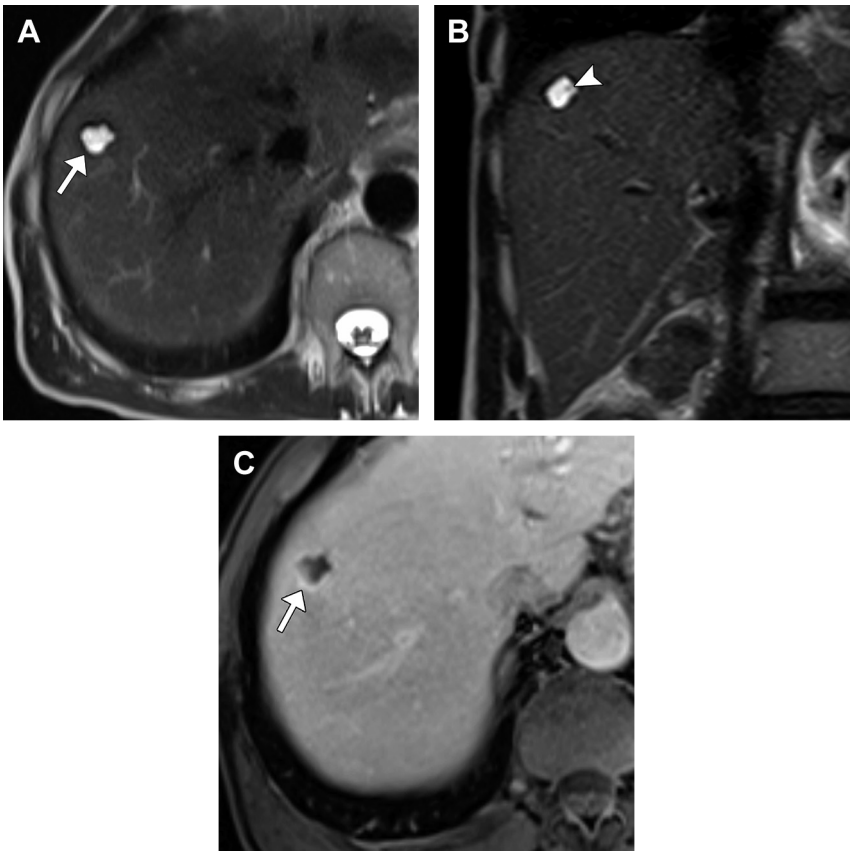

Fig. 17. Bile duct hamartoma. (*A*) Small well-defined T2 hyperintense lesion (*arrow*) with lobulated margins has a suggestion of a few thin internal septations. (*B*) Coronal T2-weighted image demonstrates a tiny mural nodule owing to conjunctive septae (*arrowhead*), a finding proposed to increase diagnostic specificity of BDH. (*C*) Postcontrast image shows a characteristic thin rim of enhancement (*arrow*).

obstruction.[96,97] Occasionally, they are asymptomatic and discovered incidentally.

On imaging studies, BCAs usually appear as large, well-defined multilobulated intrahepatic cystic masses with internal septae (**Fig. 18**). Infrequently, they appear unilocular at imaging. BCAs are typically T2 hyperintense and show variable T1 signal intensity due to proteinaceous content or blood products (**Fig. 19**).[93,98] Fluid-fluid levels occasionally result.[97,98] Frahm and colleagues[99] reported a more unusual case of BCA with multiple intracystic masses on T2-weighted images representing large blood clots floating in hemorrhagic cystic fluid. Compared with CT, MR imaging can better evaluate the relationship of the mass to the bile ducts and also can help detect the unusual case of intraductal tumoral extension.[97] MR imaging also can better demonstrate enhancement of the capsule, septae, and any mural nodules.[100] Mural or septal nodularity increases the likelihood of malignancy.[93,95,101]

It can be difficult to differentiate BCA and its malignant counterpart biliary cystadenocarcinoma (BCAC) preoperatively, but this is usually unnecessary because both require complete surgical excision. Subtotal excision or treatments reserved for simple cysts (ie, aspiration, drainage, or marsupialization) result in near universal recurrence and occasional malignant transformation.[96] The differential diagnosis includes other lesions that appear septated or multilobulated. Liver abscesses usually have thicker walls at MR imaging[98] and are associated with clinical and/or laboratory signs of infection. Hydatid cysts occur in endemic regions and are characterized by the development of daughter cysts in their periphery.[61] A cystic metastasis or rare cystic HCC may appear similar, but underlying primary malignancy or cirrhosis are usually known. Embryonal sarcoma of the liver is an unusual tumor that predominately affects children but can affect adults as well; it can mimic a complicated cystic lesion such as BCA owing to

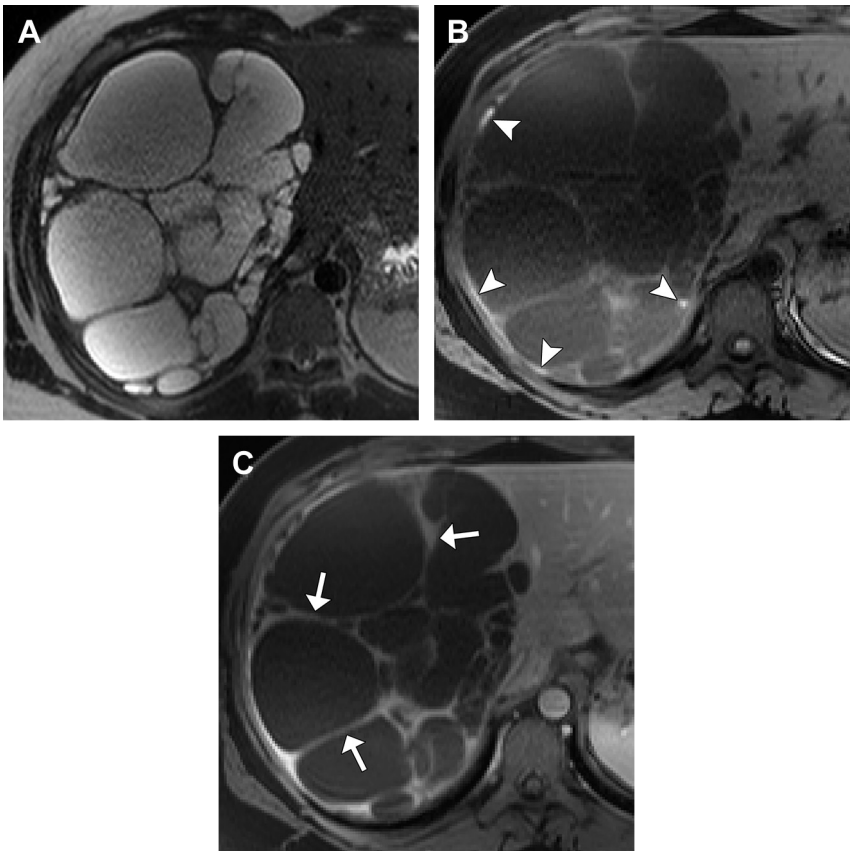

Fig. 18. Biliary cystadenoma. (*A*) Large T2 hyperintense cystic mass has multiple thick septations resulting in a multilocular appearance. (*B*) Small peripheral foci of T1 hyperintense signal on precontrast images reflect hemorrhage or proteinaceous material (*arrowheads*). (*C*) Postcontrast images demonstrate enhancement of the septae (*arrows*) and outer capsule. Multiloculated biliary cystadenoma was confirmed at resection.

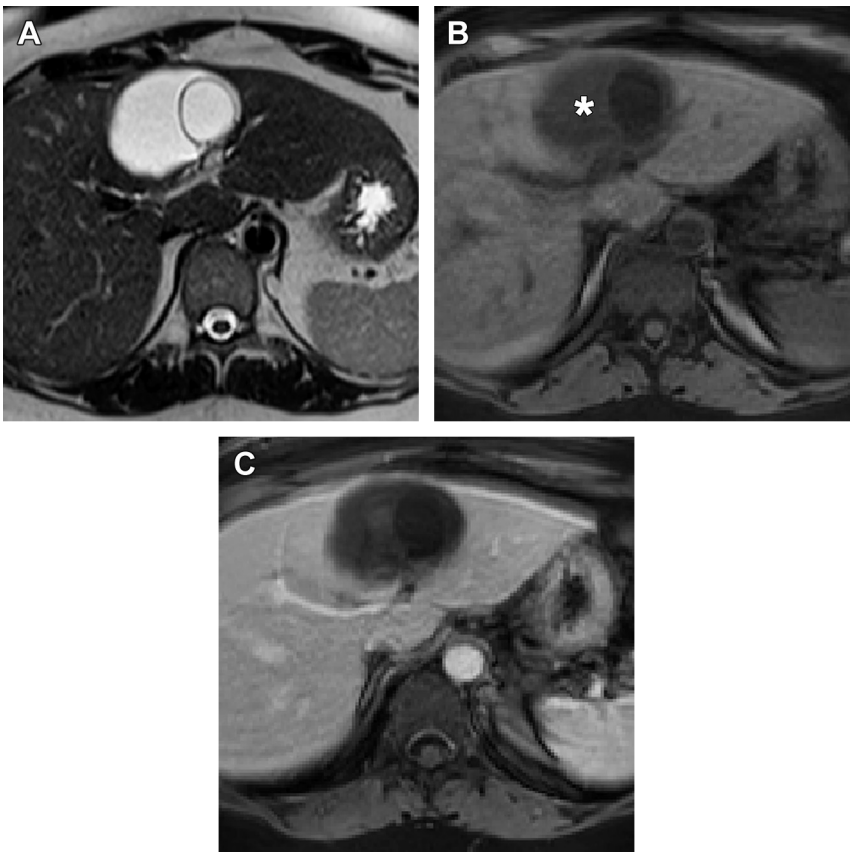

Fig. 19. Mucinous biliary cystadenoma. (*A*) T2 hyperintense cystic lesion contains a smaller eccentric internal cystic component or daughter cyst. (*B*) The larger component is of slightly greater T1 signal intensity reflecting proteinaceous material (*asterisk*). (*C*) Postcontrast imaging demonstrates no enhancing components. Mucinous biliary cystadenoma was found at surgery.

its misleading T2-hyperintense signal created by abundant myxoid stroma.[102,103]

SUMMARY

Focal liver lesions are commonly encountered during routine imaging studies. MR imaging plays an important role in the workup of the otherwise indeterminate lesion, and often can be definitive in characterization. It is important to consider the characteristic MR imaging features of benign focal hepatic lesions so as to avoid biopsy, surgery, and extensive workups. Advances in MR imaging technology and in some cases, a better understanding of the lesion itself, have allowed for improved lesion diagnosis.

REFERENCES

1. American College of Radiology. ACR Appropriateness Criteria®: liver lesion — initial characterization. Available at: http://www.acr.org/Quality-Safety/Appropriateness-Criteria/Diagnostic/~/media/ACR/Documents/AppCriteria/Diagnostic/LiverLesionInitialCharacterization.pdf. Accessed July 6, 2013.
2. Fidler J, Hough D. Hepatocyte-specific magnetic resonance imaging contrast agents. Hepatology 2011;53(2):678–82.
3. Seale MK, Catalano OA, Saini S, et al. Hepatobiliary-specific MR contrast agents: role in imaging the liver and biliary tree. Radiographics 2009;29(6):1725–48.
4. Ringe KI, Husarik DB, Sirlin CB, et al. Gadoxetate disodium-enhanced MRI of the liver: part 1, protocol optimization and lesion appearance in the noncirrhotic liver. AJR Am J Roentgenol 2010;195(1):13–28.
5. Tanimoto A, Lee JM, Murakami T, et al. Consensus report of the 2nd International Forum for Liver MRI. Eur Radiol 2009;19(Suppl 5):S975–89.
6. Koh DM, Collins DJ. Diffusion-weighted MRI in the body: applications and challenges in oncology. AJR Am J Roentgenol 2007;188(6):1622–35.
7. Taouli B, Koh DM. Diffusion-weighted MR imaging of the liver. Radiology 2010;254(1):47–66.

8. Okada Y, Ohtomo K, Kiryu S, et al. Breath-hold T2-weighted MRI of hepatic tumors: value of echo planar imaging with diffusion-sensitizing gradient. J Comput Assist Tomogr 1998;22(3):364–71.
9. Hussain SM, De Becker J, Hop WC, et al. Can a single-shot black-blood T2-weighted spin-echo echo-planar imaging sequence with sensitivity encoding replace the respiratory-triggered turbo spin-echo sequence for the liver? An optimization and feasibility study. J Magn Reson Imaging 2005;21(3):219–29.
10. Parikh T, Drew SJ, Lee VS, et al. Focal liver lesion detection and characterization with diffusion-weighted MR imaging: comparison with standard breath-hold T2-weighted imaging. Radiology 2008;246(3):812–22.
11. Taouli B, Vilgrain V, Dumont E, et al. Evaluation of liver diffusion isotropy and characterization of focal hepatic lesions with two single-shot echo-planar MR imaging sequences: prospective study in 66 patients. Radiology 2003;226(1):71–8.
12. Bruegel M, Holzapfel K, Gaa J, et al. Characterization of focal liver lesions by ADC measurements using a respiratory triggered diffusion-weighted single-shot echo-planar MR imaging technique. Eur Radiol 2008;18(3):477–85.
13. Miller FH, Hammond N, Siddiqi AJ, et al. Utility of diffusion-weighted MRI in distinguishing benign and malignant hepatic lesions. J Magn Reson Imaging 2010;32(1):138–47.
14. Agnello F, Ronot M, Valla DC, et al. High-b-value diffusion-weighted MR imaging of benign hepatocellular lesions: quantitative and qualitative analysis. Radiology 2012;262(2):511–9.
15. Cieszanowski A, Anysz-Grodzicka A, Szeszkowski W, et al. Characterization of focal liver lesions using quantitative techniques: comparison of apparent diffusion coefficient values and T2 relaxation times. Eur Radiol 2012;22(11):2514–24.
16. Caseiro-Alves F, Brito J, Araujo AE, et al. Liver haemangioma: common and uncommon findings and how to improve the differential diagnosis. Eur Radiol 2007;17(6):1544–54.
17. Doyle DJ, Khalili K, Guindi M, et al. Imaging features of sclerosed hemangioma. AJR Am J Roentgenol 2007;189(1):67–72.
18. Vilgrain V, Uzan F, Brancatelli G, et al. Prevalence of hepatic hemangioma in patients with focal nodular hyperplasia: MR imaging analysis. Radiology 2003;229(1):75–9.
19. Markovic MV, Petricusic L, Curic J, et al. Magnetic resonance imaging of chronic bleeding into a giant hepatic hemangioma. Eur J Radiol Extra 2011;77:e9–11.
20. Vilgrain V, Boulos L, Vullierme MP, et al. Imaging of atypical hemangiomas of the liver with pathologic correlation. Radiographics 2000;20(2):379–97.
21. Danet IM, Semelka RC, Braga L, et al. Giant hemangioma of the liver: MR imaging characteristics in 24 patients. Magn Reson Imaging 2003;21(2):95–101.
22. Jang HJ, Kim TK, Lim HK, et al. Hepatic hemangioma: atypical appearances on CT, MR imaging, and sonography. AJR Am J Roentgenol 2003;180(1):135–41.
23. Jeong MG, Yu JS, Kim KW. Hepatic cavernous hemangioma: temporal peritumoral enhancement during multiphase dynamic MR imaging. Radiology 2000;216(3):692–7.
24. Prasanna PM, Fredericks SE, Winn SS, et al. Best cases from the AFIP: giant cavernous hemangioma. Radiographics 2010;30(4):1139–44.
25. Jhaveri KS, Vlachou PA, Guindi M, et al. Association of hepatic hemangiomatosis with giant cavernous hemangioma in the adult population: prevalence, imaging appearance, and relevance. AJR Am J Roentgenol 2011;196(4):809–15.
26. Silva AC, Evans JM, McCullough AE, et al. MR imaging of hypervascular liver masses: a review of current techniques. Radiographics 2009;29(2):385–402.
27. Doo KW, Lee CH, Choi JW, et al. "Pseudo washout" sign in high-flow hepatic hemangioma on gadoxetic acid contrast-enhanced MRI mimicking hypervascular tumor. AJR Am J Roentgenol 2009;193(6):W490–6.
28. Goshima S, Kanematsu M, Watanabe H, et al. Hepatic hemangioma and metastasis: differentiation with gadoxetate disodium-enhanced 3-T MRI. AJR Am J Roentgenol 2010;195(4):941–6.
29. Marin D, Brancatelli G, Federle MP, et al. Focal nodular hyperplasia: typical and atypical MRI findings with emphasis on the use of contrast media. Clin Radiol 2008;63(5):577–85.
30. Mortele KJ, Praet M, Van Vlierberghe H, et al. CT and MR imaging findings in focal nodular hyperplasia of the liver: radiologic-pathologic correlation. AJR Am J Roentgenol 2000;175(3):687–92.
31. Scalori A, Tavani A, Gallus S, et al. Oral contraceptives and the risk of focal nodular hyperplasia of the liver: a case-control study. Am J Obstet Gynecol 2002;186(2):195–7.
32. Scott LD, Katz AR, Duke JH, et al. Oral contraceptives, pregnancy, and focal nodular hyperplasia of the liver. JAMA 1984;251(11):1461–3.
33. Mathieu D, Kobeiter H, Maison P, et al. Oral contraceptive use and focal nodular hyperplasia of the liver. Gastroenterology 2000;118(3):560–4.
34. Buetow PC, Pantongrag-Brown L, Buck JL, et al. Focal nodular hyperplasia of the liver: radiologic-pathologic correlation. Radiographics 1996;16(2):369–88.
35. Hussain SM, Terkivatan T, Zondervan PE, et al. Focal nodular hyperplasia: findings at state-of-the-art MR

imaging, US, CT, and pathologic analysis. Radiographics 2004;24(1):3–17 [discussion: 18–9].
36. Chaoui A, Mergo PJ, Lauwers GY. Unusual appearance of focal nodular hyperplasia with fatty change. AJR Am J Roentgenol 1998; 171(5):1433–4.
37. Grazioli L, Morana G, Federle MP, et al. Focal nodular hyperplasia: morphologic and functional information from MR imaging with gadobenate dimeglumine. Radiology 2001;221(3):731–9.
38. Blachar A, Federle MP, Ferris JV, et al. Radiologists' performance in the diagnosis of liver tumors with central scars by using specific CT criteria. Radiology 2002;223(2):532–9.
39. International Working Party. Terminology of nodular hepatocellular lesions. Hepatology 1995;22:11.
40. McLarney JK, Rucker PT, Bender GN, et al. Fibrolamellar carcinoma of the liver: radiologic-pathologic correlation. Radiographics 1999;19(2): 453–71.
41. Hamrick-Turner JE, Shipkey FH, Cranston PE. Fibrolamellar hepatocellular carcinoma: MR appearance mimicking focal nodular hyperplasia. J Comput Assist Tomogr 1994;18(2):301–4.
42. van Kessel CS, de Boer E, Kate FJ, et al. Focal nodular hyperplasia: hepatobiliary enhancement patterns on gadoxetic-acid contrast-enhanced MRI. Abdom Imaging 2013;38(3):490–501.
43. Karam AR, Shankar S, Surapaneni P, et al. Focal nodular hyperplasia: central scar enhancement pattern using gadoxetate disodium. J Magn Reson Imaging 2010;32(2):341–4.
44. Laumonier H, Bioulac-Sage P, Laurent C, et al. Hepatocellular adenomas: magnetic resonance imaging features as a function of molecular pathological classification. Hepatology 2008;48(3):808–18.
45. Ronot M, Bahrami S, Calderaro J, et al. Hepatocellular adenomas: accuracy of magnetic resonance imaging and liver biopsy in subtype classification. Hepatology 2011;53(4):1182–91.
46. Katabathina VS, Menias CO, Shanbhogue AK, et al. Genetics and imaging of hepatocellular adenomas: 2011 update. Radiographics 2011;31(6):1529–43.
47. Grazioli L, Federle MP, Brancatelli G, et al. Hepatic adenomas: imaging and pathologic findings. Radiographics 2001;21(4):877–92 [discussion: 892–4].
48. Furlan A, van der Windt DJ, Nalesnik MA, et al. Multiple hepatic adenomas associated with liver steatosis at CT and MRI: a case-control study. AJR Am J Roentgenol 2008;191(5):1430–5.
49. Flejou JF, Barge J, Menu Y, et al. Liver adenomatosis. An entity distinct from liver adenoma? Gastroenterology 1985;89(5):1132–8.
50. Grazioli L, Federle MP, Ichikawa T, et al. Liver adenomatosis: clinical, histopathologic, and imaging findings in 15 patients. Radiology 2000;216(2): 395–402.
51. Bioulac-Sage P, Laumonier H, Couchy G, et al. Hepatocellular adenoma management and phenotypic classification: the Bordeaux experience. Hepatology 2009;50(2):481–9.
52. Paulson EK, McClellan JS, Washington K, et al. Hepatic adenoma: MR characteristics and correlation with pathologic findings. AJR Am J Roentgenol 1994;163(1):113–6.
53. Brancatelli G, Federle MP, Vullierme MP, et al. CT and MR imaging evaluation of hepatic adenoma. J Comput Assist Tomogr 2006;30(5):745–50.
54. Dokmak S, Paradis V, Vilgrain V, et al. A single-center surgical experience of 122 patients with single and multiple hepatocellular adenomas. Gastroenterology 2009;137(5):1698–705.
55. Stoot JH, Coelen RJ, De Jong MC, et al. Malignant transformation of hepatocellular adenomas into hepatocellular carcinomas: a systematic review including more than 1600 adenoma cases. HPB (Oxford) 2010;12(8):509–22.
56. van Aalten SM, Thomeer MG, Terkivatan T, et al. Hepatocellular adenomas: correlation of MR imaging findings with pathologic subtype classification. Radiology 2011;261(1):172–81.
57. Chung KY, Mayo-Smith WW, Saini S, et al. Hepatocellular adenoma: MR imaging features with pathologic correlation. AJR Am J Roentgenol 1995; 165(2):303–8.
58. Mendez RJ, Schiebler ML, Outwater EK, et al. Hepatic abscesses: MR imaging findings. Radiology 1994;190(2):431–6.
59. Chan JH, Tsui EY, Luk SH, et al. Diffusion-weighted MR imaging of the liver: distinguishing hepatic abscess from cystic or necrotic tumor. Abdom Imaging 2001;26(2):161–5.
60. Tian LT, Yao K, Zhang XY, et al. Liver abscesses in adult patients with and without diabetes mellitus: an analysis of the clinical characteristics, features of the causative pathogens, outcomes and predictors of fatality: a report based on a large population, retrospective study in China. Clin Microbiol Infect 2012;18(9):E314–30.
61. Mortele KJ, Segatto E, Ros PR. The infected liver: radiologic-pathologic correlation. Radiographics 2004;24(4):937–55.
62. Mezhir JJ, Fong Y, Jacks LM, et al. Current management of pyogenic liver abscess: surgery is now second-line treatment. J Am Coll Surg 2010; 210(6):975–83.
63. Branum GD, Tyson GS, Branum MA, et al. Hepatic abscess. Changes in etiology, diagnosis, and management. Ann Surg 1990;212(6):655–62.
64. Meddings L, Myers RP, Hubbard J, et al. A population-based study of pyogenic liver abscesses in the United States: incidence, mortality, and temporal trends. Am J Gastroenterol 2010; 105(1):117–24.

65. Foo NP, Chen KT, Lin HJ, et al. Characteristics of pyogenic liver abscess patients with and without diabetes mellitus. Am J Gastroenterol 2010; 105(2):328–35.
66. Law ST, Li KK. Is hepatic neoplasm-related pyogenic liver abscess a distinct clinical entity? World J Gastroenterol 2012;18(10):1110–6.
67. Wong WM, Wong BC, Hui CK, et al. Pyogenic liver abscess: retrospective analysis of 80 cases over a 10-year period. J Gastroenterol Hepatol 2002; 17(9):1001–7.
68. Pang TC, Fung T, Samra J, et al. Pyogenic liver abscess: an audit of 10 years' experience. World J Gastroenterol 2011;17(12):1622–30.
69. Balci NC, Semelka RC, Noone TC, et al. Pyogenic hepatic abscesses: MRI findings on T1- and T2-weighted and serial gadolinium-enhanced gradient-echo images. J Magn Reson Imaging 1999;9(2):285–90.
70. Jeffrey RB Jr, Tolentino CS, Chang FC, et al. CT of small pyogenic hepatic abscesses: the cluster sign. AJR Am J Roentgenol 1988;151(3):487–9.
71. Mathieu D, Vasile N, Fagniez PL, et al. Dynamic CT features of hepatic abscesses. Radiology 1985; 154(3):749–52.
72. Rajak CL, Gupta S, Jain S, et al. Percutaneous treatment of liver abscesses: needle aspiration versus catheter drainage. AJR Am J Roentgenol 1998;170(4):1035–9.
73. Elsayes KM, Narra VR, Yin Y, et al. Focal hepatic lesions: diagnostic value of enhancement pattern approach with contrast-enhanced 3D gradient-echo MR imaging. Radiographics 2005;25(5): 1299–320.
74. Horton KM, Bluemke DA, Hruban RH, et al. CT and MR imaging of benign hepatic and biliary tumors. Radiographics 1999;19(2):431–51.
75. Wheeler DA, Edmondson HA. Ciliated hepatic foregut cyst. Am J Surg Pathol 1984;8(6):467–70.
76. Sharma S, Dean AG, Corn A, et al. Ciliated hepatic foregut cyst: an increasingly diagnosed condition. Hepatobiliary Pancreat Dis Int 2008;7(6):581–9.
77. Kadoya M, Matsui O, Nakanuma Y, et al. Ciliated hepatic foregut cyst: radiologic features. Radiology 1990;175(2):475–7.
78. Shoenut JP, Semelka RC, Levi C, et al. Ciliated hepatic foregut cysts: US, CT, and contrast-enhanced MR imaging. Abdom Imaging 1994; 19(2):150–2.
79. Rodriguez E, Soler R, Fernandez P. MR imagings of ciliated hepatic foregut cyst: an unusual cause of fluid-fluid level within a focal hepatic lesion (2005.4b). Eur Radiol 2005;15(7):1499–501.
80. Vick DJ, Goodman ZD, Deavers MT, et al. Ciliated hepatic foregut cyst: a study of six cases and review of the literature. Am J Surg Pathol 1999; 23(6):671–7.
81. Dardik H, Glotzer P, Silver C. Congenital hepatic cyst causing jaundice: report of a case and analogies with respiratory malformations. Ann Surg 1964;159:585–92.
82. Harty MP, Hebra A, Ruchelli ED, et al. Ciliated hepatic foregut cyst causing portal hypertension in an adolescent. AJR Am J Roentgenol 1998; 170(3):688–90.
83. Vick DJ, Goodman ZD, Ishak KG. Squamous cell carcinoma arising in a ciliated hepatic foregut cyst. Arch Pathol Lab Med 1999;123(11):1115–7.
84. de Lajarte-Thirouard AS, Rioux-Leclercq N, Boudjema K, et al. Squamous cell carcinoma arising in a hepatic forgut cyst. Pathol Res Pract 2002;198(10):697–700.
85. Furlanetto A, Dei Tos AP. Squamous cell carcinoma arising in a ciliated hepatic foregut cyst. Virchows Arch 2002;441(3):296–8.
86. Zhang X, Wang Z, Dong Y. Squamous cell carcinoma arising in a ciliated hepatic foregut cyst: case report and literature review. Pathol Res Pract 2009;205(7):498–501.
87. Kimura A, Makuuchi M, Takayasu K, et al. Ciliated hepatic foregut cyst with solid tumor appearance on CT. J Comput Assist Tomogr 1990;14(6):1016–8.
88. Tohme-Noun C, Cazals D, Noun R, et al. Multiple biliary hamartomas: magnetic resonance features with histopathologic correlation. Eur Radiol 2008; 18(3):493–9.
89. Lev-Toaff AS, Bach AM, Wechsler RJ, et al. The radiologic and pathologic spectrum of biliary hamartomas. AJR Am J Roentgenol 1995;165(2):309–13.
90. Martin DR, Kalb B, Sarmiento JM, et al. Giant and complicated variants of cystic bile duct hamartomas of the liver: MRI findings and pathological correlations. J Magn Reson Imaging 2010;31(4):903–11.
91. Zheng RQ, Zhang B, Kudo M, et al. Imaging findings of biliary hamartomas. World J Gastroenterol 2005;11(40):6354–9.
92. Semelka RC, Hussain SM, Marcos HB, et al. Biliary hamartomas: solitary and multiple lesions shown on current MR techniques including gadolinium enhancement. J Magn Reson Imaging 1999; 10(2):196–201.
93. Buetow PC, Buck JL, Pantongrag-Brown L, et al. Biliary cystadenoma and cystadenocarcinoma: clinical-imaging-pathologic correlations with emphasis on the importance of ovarian stroma. Radiology 1995;196(3):805–10.
94. Ishak KG, Willis GW, Cummins SD, et al. Biliary cystadenoma and cystadenocarcinoma: report of 14 cases and review of the literature. Cancer 1977;39(1):322–38.
95. Korobkin M, Stephens DH, Lee JK, et al. Biliary cystadenoma and cystadenocarcinoma: CT and sonographic findings. AJR Am J Roentgenol 1989;153(3):507–11.

96. Thomas KT, Welch D, Trueblood A, et al. Effective treatment of biliary cystadenoma. Ann Surg 2005; 241(5):769–73 [discussion: 773–5].
97. Baudin G, Novellas S, Buratti MS, et al. Atypical MRI features of a biliary cystadenoma revealed by jaundice. Clin Imaging 2006;30(6):413–5.
98. Lewin M, Mourra N, Honigman I, et al. Assessment of MRI and MRCP in diagnosis of biliary cystadenoma and cystadenocarcinoma. Eur Radiol 2006; 16(2):407–13.
99. Frahm C, Zimmermann A, Heller M, et al. Uncommon presentation of a giant biliary cystadenoma: correlation between MRI and pathologic findings. J Magn Reson Imaging 2001;14(5): 649–52.
100. Williams DM, Vitellas KM, Sheafor D. Biliary cystadenocarcinoma: seven year follow-up and the role of MRI and MRCP. Magn Reson Imaging 2001;19(9):1203–8.
101. Choi BI, Lim JH, Han MC, et al. Biliary cystadenoma and cystadenocarcinoma: CT and sonographic findings. Radiology 1989;171(1):57–61.
102. Buetow PC, Buck JL, Pantongrag-Brown L, et al. Undifferentiated (embryonal) sarcoma of the liver: pathologic basis of imaging findings in 28 cases. Radiology 1997;203(3):779–83.
103. Tsukada A, Ishizaki Y, Nobukawa B, et al. Embryonal sarcoma of the liver in an adult mimicking complicated hepatic cyst: MRI findings. J Magn Reson Imaging 2010;31(6):1477–80.